Materials Advances

ROYAL SOCIETY OF CHEMISTRY

REVIEW

View Article Online
View Journal | View Issue

Cite this: *Mater. Adv.*, 2023, 4, 6152

Recent advances in Ni-materials/carbon nanocomposites for supercapacitor electrodes

Ghobad Behzadi Pour, *[a] Hamed Nazarpour Fard,[b] Leila Fekri Aval [c] and Deepak Dubal[d]

Recent advancements in Ni material-based supercapacitors have focused on their composites with carbon nanomaterials. These composites demonstrate improved electrical conductivity, enhanced surface area, and superior electrochemical performance by addressing critical issues related to cycling stability and low energy density. This review provides an overview of Ni material-based carbon nanocomposites including graphene (Ni/graphene), carbon nanotubes (Ni/CNTs), and activated carbon (Ni/AC) as potential electrodes for supercapacitors. The synergistic effects of Ni and carbon in nanocomposites on electrochemical properties such as capacitance, cycling stability, and specific capacitance are systematically outlined. The findings will serve as a valuable resource for understanding the structure–property–performance relationship of Ni-based composite materials for energy storage applications.

Received 28th August 2023,
Accepted 3rd November 2023

DOI: 10.1039/d3ma00609c

rsc.li/materials-advances

1. Introduction

The development of stationary and automotive systems requires effective and efficient energy storage devices. Supercapacitors were introduced as promising energy storage systems due to their high-power density and long cycle life. Recently, the development of supercapacitors has mostly focused on increasing their energy density by fabricating advanced electrode materials and electrolytes. Ni materials are highly regarded in the realm of supercapacitors due to their remarkable electrochemical properties including long cycle life, fast charge/discharge rates, and high specific capacity. Ni material supercapacitors find wide applications in energy storage systems, hybrid vehicles, portable electronics, and renewable energy systems. Fig. 1 shows the advantages of supercapacitors and the properties of carbon nanomaterials as an electrode of supercapacitors. Also, different types of Ni materials/carbon nanomaterials supercapacitors are shown in Fig. 1.

The choice of materials for supercapacitor electrodes plays a critical role in determining the performance and characteristics. Some of the common types of materials used in supercapacitor electrodes are activated carbon, CNTs, graphene, metal oxides, conducting polymers, transition metal carbides, carbon aerogels, and hybrids and composites. Ni itself is a good conductor of electricity, which allows for rapid electron transport within the electrode material. Some Ni-based materials, such as nickel hydroxide, exhibit pseudocapacitance. This property leads to higher specific capacitance and overall energy storage capacity. Ni is a relatively abundant and cost-effective material compared to precious metals, is eco-friendly, easy to use in manufacturing processes, and has good stability and longevity. Ni-based materials can be combined with other substances to form composites or hybrid electrodes. This versatility enables researchers to develop supercapacitor electrodes. The composite of Ni materials with carbon nanomaterials in supercapacitors improves performance by enhancing conductivity, increasing surface area, improving stability, facilitating ion diffusion, and leveraging synergistic effects between the materials. These improvements contribute to higher energy storage capacity, faster charging/discharging rates, and improved overall device performance.[1–5] Fig. 2 shows the cumulative growth of published articles in recent years on Ni material supercapacitors. During the last decade, the growth of scientific research on using nickel materials to fabricate supercapacitor electrodes has increased significantly. The cumulative number of scientific studies has reached more than 3000 published articles, of which about 71% are from China, 10% from India, 9% from South Korea, 5% from the United States, and the share of other countries is 5%. Co-occurrence analysis is the way to investigate using keywords. In this analysis, the information related to the relationship between

[a] *Department of Physics, East Tehran Branch, Islamic Azad University, Tehran, Iran. E-mail: ghobadbehzadi@yahoo.com; Tel: +989120345348*
[b] *Department of Polymer Engineering, Faculty of Engineering, Lorestan University, Khoram-Abad, Iran. E-mail: nazarpoorfard@gmail.com*
[c] *Quantum Technologies Research Center, Science and Research Branch, Islamic Azad University, Tehran, Iran. E-mail: leila2mst@yahoo.com*
[d] *School of Chemistry and Physics, Queensland University of Technology (QUT), George Street, Brisbane, QLD 4001, Australia. E-mail: deepak.dubal@qut.edu.au*

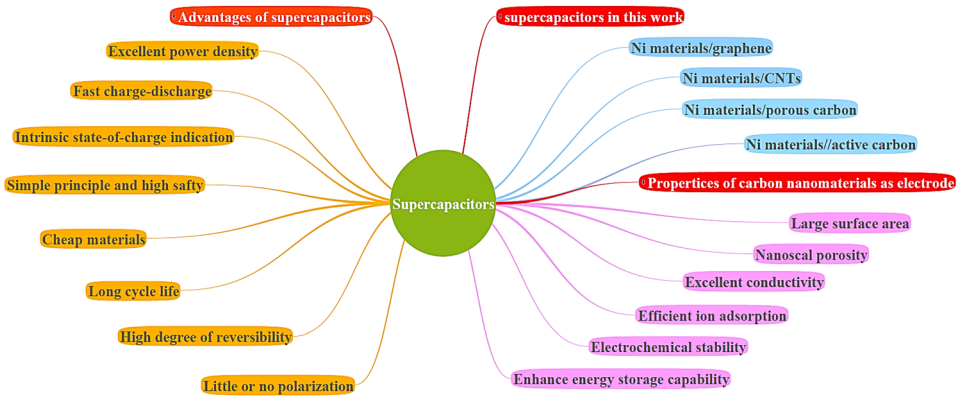

Fig. 1 Advantages of supercapacitors and the properties of carbon nanomaterials as an electrode of supercapacitors.

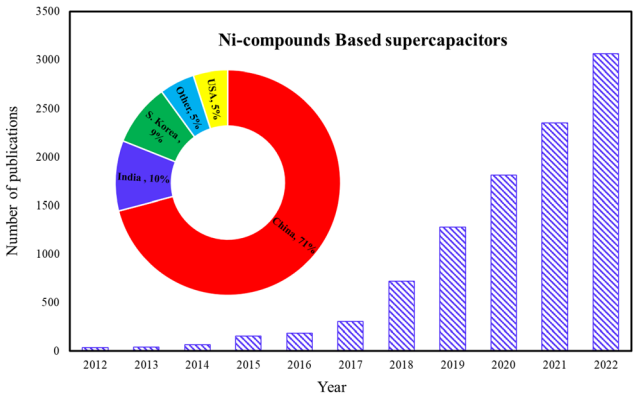

Fig. 2 The cumulative growth in Ni material-based supercapacitor publications.

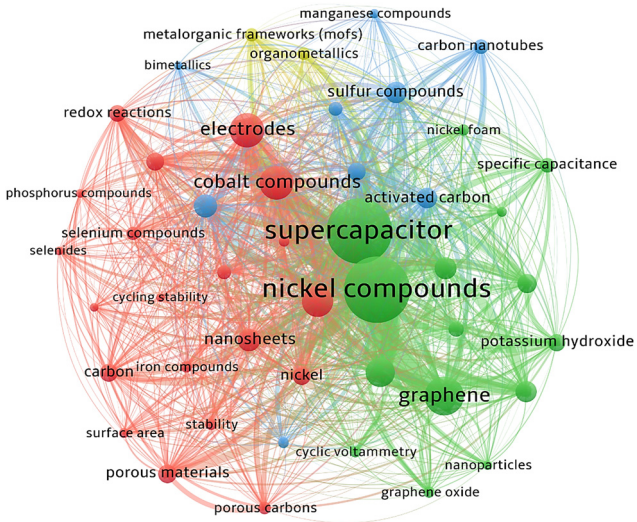

Fig. 3 Co-occurrence keyword analysis of Ni material-based supercapacitors using VOSviewer.

keywords in different reports, the amount of repetition of keywords, and the identification of different materials in the fabrication of supercapacitor electrodes that use nickel materials in their structure can be obtained. The VOSviewer image of Ni material-based supercapacitors from Scopus for 2022–2023 publications is shown in Fig. 3.

As shown in Fig. 3, electrodes based on Ni materials and carbon nanomaterials are prominent keywords. Recently, nanocomposites of Ni materials with carbon nanomaterials as supercapacitor electrodes such as $NiCo_2S_4$/graphene,[6] $Ni(OH)_2$/graphene,[7] $NiCo_2O_4$/graphene,[8,9] Ni–Co/graphene,[10–17] $NiMoO_4$/graphene,[18–20] $Ni(OH)_2$/CNTs,[21,22] Ni–Co/CNTs,[23–25] $NiCo_2S_4$/CNTs,[26–29] Ni–Co/porous carbon,[30] $NiCo_2S_4$/porous carbon,[31] $NiCo_2O_4$//AC,[32] Ni–Co//AC,[33–36] $Ni(OH)_2$//AC,[37] and other materials have been developed.

$NiCo_2S_4$ due to its high electrochemical stability offers advantages such as good cycling stability, and compatibility with flexible devices. Their primary components are widely available, making them cost-effective. $NiCo_2S_4$/carbon nanomaterial electrodes combine the advantages of $NiCo_2S_4$ and carbon nanomaterials to enhance energy storage. The synergy of both materials results in an improved power density and faster charge rates.[38–43] $NiCo_2O_4$ belongs to the class of transition metal oxides and exhibits favorable electrochemical properties. Additionally, the properties of $NiCo_2O_4$ can be tuned by adjusting its synthesis parameters, allowing for optimization of its electrochemical performance to meet specific application requirements. The key distinction between $NiCo_2O_4$ and $NiCo_2S_4$-based supercapacitors lies in the redox reactions occurring at the electrode material. $NiCo_2O_4$ undergoes redox reactions involving oxygen atoms, while $NiCo_2S_4$ involves sulfur atoms. Recently, several kinds of research have been reported on supercapacitors based on $NiCo_2O_4$/carbon nanomaterials.[44–48] $Ni(OH)_2$-based supercapacitors are widely used due to efficient charge storage and are environmentally friendly. In supercapacitors based on $Ni(OH)_2$/carbon nanomaterials, the performance characteristics are improved.[49–54] The specific capacitance, power density, energy density, and cycle stability are important parameters in the classification of supercapacitors. Cycle stability refers to their ability to maintain a consistent performance over repeated charge and discharge cycles without significant degradation. It involves

mitigating factors such as capacitance loss, resistance increase, leakage current, and mechanical stress. These degradation mechanisms can impact the specific capacitance, power delivery, and overall efficiency of the supercapacitor.[55,56] Wu *et al.*[57] reported a supercapacitor based on Ni_3Se_4@Co_3Se_4-1 : 3//rGO-Zn electrodes with a specific capacitance of 1120 F g^{-1}. Ternary nanocomposites of nickel molybdate/reduced graphene oxide/polypyrrole ($NiMoO_4$/rGO/PPy), as a supercapacitor electrode were investigated in ref. 58 This paper mentioned that with $NiMoO_4$/rGO-450/PPy@NF//AC/graphite@NF electrodes, the energy and power densities of the supercapacitor were 43.65 W h kg^{-1} and 600 W kg^{-1}, respectively. In another study, a supercapacitor based on $FeNiS_2$ nanosheets decorated on rGO showed a specific capacitance of 1013 F g^{-1}.[59] Flexible supercapacitors play a significant role in soft, wearable, and portable electronics. Li *et al.*[60] investigated a $CoNiP_2O_7$/CNT nanocomposite as a positive electrode for micro-supercapacitors. They obtained an areal capacitance of 20.9 mF cm^{-2} at 0.08 mA cm^{-2} and an energy density of 2.9 μW h cm^{-2}. A supercapacitor based on the MWCNTs@Ni_3S_2/Cu_xS electrode presented a specific capacitance of 1388.7 F g^{-1} using the galvanostatic charge–discharge method and cycling stability of 100% after 10 000 cycles.[61] $Ni_3P_2O_8$ nanodot anchored MWCNT nanocomposites as a supercapacitor electrode were reported in ref. 62 This structure achieved a specific energy of 72.3 W h kg^{-1} with a power density of 6.4 kW kg^{-1}. Recent research on Ni materials and porous carbon nanocomposites as electrodes has shown good progress.[63–68] Nanomaterials and nanocomposites are receiving more attention in making energy storage devices, sensors, and different applications.[69–75] In this review, the developments of Ni material/carbon nanomaterial-based supercapacitors for 2022–2023 publications (Scopus) are studied and compared. We have discussed the specific capacitance, power density, energy density, cycling stability, and rate capability of Ni-materials/carbon nanocomposites in supercapacitor applications. This article provides valuable insights into the introduction and development of recent Ni-based supercapacitors with high performance. It serves as a comprehensive resource for researchers and engineers working in the field of energy storage, facilitating further advancements in the design of efficient and sustainable energy storage systems.

2. Materials manufacturing for supercapacitors

2.1. Graphene-based supercapacitors

Various nanocomposites containing Ni and graphene have been frequently employed in supercapacitor and electrochemical applications and the novel results from the reported papers are tabulated in Table 1. From Table 1 the specific capacitance of Ni-materials/graphene-based supercapacitors is obtained, which is shown in Fig. 4. As can be seen from Fig. 4 the specific capacitance of Ni-materials/graphene-based supercapacitors reached 3268 F g^{-1}. For better comparison, the energy density as a function of power density is also plotted in Fig. 4. From Fig. 4 the power density of most Ni-materials/graphene-based supercapacitors is less than 2 KW kg^{-1} and the energy density is less than 100 W h kg^{-1}.

The specific capacitance of the $NiMoO_4$/rGO composite reached 2056 F g^{-1} at a current density of 2 A g^{-1}. Using $NiMoO_4$/rGO as the (+) electrode in supercapacitors combined with AC as the (−) electrode led to the high-power density.[76] $ZnFe_2O_4$/$NiMoO_4$ nanosheet/rGO-NF as the cathode and MOF-derived hollow porous carbon as the anode was used in the supercapacitor leading to a high energy density of 58.6 W h kg^{-1} at a power density of 799 W kg^{-1} with prolonged cycling.[77] Polyaniline/$NiFe_2O_4$/rGO hydrogel nanocomposites on carbon cloth showed high characteristics that led to the high properties in the corresponding supercapacitors attributed to its well-designed 3D microstructure and diffusion-controlled mechanism.[78] Also, rGO/$NiFe_2O_4$ exhibited high electrochemical characteristics including a high specific capacity of 1320 C g^{-1} as well as high characteristics in the corresponding supercapacitor.[79]

Porous CuNi phosphide spheres/rGO as the cathode electrode have advantages such as fast electrolyte diffusion, better electron transfer, and better structural stability. Its supercapacitor with AC-anode represented a satisfactory energy density.[80,81] The 450 °C annealed nanocomposite of $NiMoO_4$/rGO-450/polypyrrole exhibited a specific capacitance of 1805 F g^{-1}. $NiCoSe_4$/N-rGO were fabricated using a solvothermal method and $NiCoSe_4$/N-rGO-20 presents a specific capacity of 120 mA h g^{-1}. The $NiCoSe_4$/N-rGO-20 (anode)//N-rGO (cathode) supercapacitor demonstrated an ultra-high energy density of 14 W h kg^{-1} and good circulation stability.[82] The spongy nanocomposite of $CoNi_2S_4$//MoS_2/rGO has a specific capacitance of 3268 F g^{-1} at 1.0 A g^{-1}. Its use in supercapacitors led to the optimal potential window and the high energy density of 41 W h kg^{-1}.[83] rGO/Ni_2ZnS_4 was used as a cathode material with a specific capacitance of 1150 F g^{-1}. The capacitor composed of AC//rGO/Ni_2ZnS_4-1.5 h has an energy density of 31.06 W h kg^{-1}.[84] Spinel Ni cobaltite nanoflowers/rGO as an electrode material demonstrated a specific capacitance of 2695 F g^{-1} at 1 A g^{-1} and also exhibited a maximum energy density of 93.57 W h kg^{-1}.[85] The chalcogen-modified Ni–Mo selenide/rGO composites indicated that the Se-based electrode revealed the highest electrochemical properties. Also, a supercapacitor of this (+) electrode and thermally rGO electrode (−) presented a maximum energy density of 60.5 W h kg^{-1}.[86] $NiSe_2$/rGO with various rGO weight ratios were fabricated and the $NiSe_2$ (16%) rGO electrode outperformed the others due to its interconnected network topology and decreased effect of volume expansions. A supercapacitor with $NiSe_2$-16% rGO (anode) and AC (cathode) exhibited a high retention of capacitance and energy density of 12.66 W h kg^{-1}.[87] Nanorod Ni-MOF-74 derived NiSe nanoparticles/rGO have been successfully prepared (NiSe/rGO) and showed an improved electrochemical performance so that the supercapacitor of NiSe/rGO (+)//(−) AC delivered energy density of 52.8 W h kg^{-1} and outstanding long-term cycling retention.[88] The optimized rGO/polyaniline/$NiMoS_4$ electrode exhibited a high specific capacitance of

Table 1 The electrochemical results collected from various studies done on Ni/graphene nanocomposites

Electrode material	Capacitance retention (CR%/Cycle)	Specific capacitance ($F\ g^{-1}$)	Energy density ($W\ h\ kg^{-1}$)	Power density ($W\ kg^{-1}$)	Ref.
$NiMoO_4$/rGO	91.1/1000	2056	60.2	750.2	76
$NiMoO_4$/rGO–Ni/$ZnFe_2O_4$	89.6/7000	—	58.6	799	77
$NiFe_2O_4$/rGO/polyaniline	—	1134.28	19.29	610	78
$NiFe_2O_4$/rGO	94/5000	1320 C g^{-1}	75	2343	79
Ni–Cu/rGO	91.8/13 000	1075 C g^{-1}	64	801	80
Ni molybdate/rGO	—	1805	43.65	600	81
$NiCoSe_4$/rGO	93/5000	120 mA h g^{-1}	14	902	82
$CoNi_2S_4$/rGO/MoS_2	—	3268	41	700	83
Ni_2ZnS_4/rGO/ZIF-8	59.7/2000	1150	31.06	750.44	84
Ni cobaltite/rGO	96/2500	2695	93.57	250	85
Ni–Mo/rGO	83.4/—	1220	60.5	1470	86
$NiSe_2$/rGO	99/8000	1845.5	12.66	3999.84	87
NiSe/rGO	90/5000	781 C g^{-1}	52.8	930	88
$NiMoS_4$/rGO/polyaniline	93/6000	194 mA h g^{-1}	30.75	1500	89
NiSe/rGO/C	75/5000	448.9 mA h g^{-1}	60.5	13 340	90
$NiSe_2$/rGO	78.13/5000	224.75 mA h g^{-1}	25.85	730	91
Ni_3S_2/rGO	95.4/10 000	1960 mF cm^{-2}	67.9	535.7	92
$NiCoO_2$/rGO/MXene	77.29/10 000	1614	45.15	394.52	93
Ni/rGO	70/—	52.64 mA h g^{-1}	18.72	547.52	94
Ni/graphene	—	1900	37	5000	95
Ni phosphide/graphene	85.2/10 000	1338.8	33.4	792.1	96
Ni/GO	92.5/10 000	1115.6	52.5	18 000	97
Ni–Fe/graphene	—	1541 mA h g^{-1}	190	9600	98
$NiWO_3$/GO/PANI	92.6/10 000	1380	47.8	—	99
NiGa/graphene quantum dots	87.5/5000	2160	78.8	1432.7	100
Ni–Co/rGO	—	1913.5	59.2	750	103
Ni–Co/Co_3O_4/graphene	99.8/10 500	1866	66.7	800	104
Ni–Co phosphide/rGO	90/10 000	2384	39.7	8820	105
Ni–Co selenide/rGO	80.8/5000	2009	38	388	106
Ni–Co selenide/graphene	84.6/5000	421.3 C g^{-1}	40.4	533.3	107
Ni–Co sulfide/MnS/rGO	83.6/10 000	1248 C g^{-1}	42.0	793.8	108
Ni–Co/graphene	89.6/10 000	1740	41.6	750	109
Ni–Co/graphene	83.2/10 200	—	40.6	400	110
Ni–Co/rGO	87.3/10 000	2137.8	54.25	750	111
Ni–Co/N-GH/NF//GH/CNT	—	209	63.33	260	112
Ni–Co/rGO/MXene	70.87/10 000	248.13 mA h g^{-1}	29.46	700.34	113
Ni–Co/rGO	85.1/10 000	582.1 mA h g^{-1}	56.0	515.0	114
Ni–Co/graphene quantum dots	86.2/8000	1628	46	7440	115
Ni–Co/MWCNTs–GO	91.92/10 000	2532.80	77.61	850	116
Ni–Co/rGO	75.5/5000	2020 mF cm^{-2}	117.3 μW h cm^{-2}	34 000 μW cm^{-2}	117
$NiCo_2S_4$/rGO/g-C_3N_4	93.6/6000	1938	66	751	120
$NiCo_2S_4$/graphene	—	1325.9	30.72	1280	121
$NiCo_2S_4$/graphene/Ni–Mo	80/10 000	1346	59.38	808.19	122
$NiCo_2S_4$/rGO/CoNi	80.52/10 000	1846.66	28.88	—	123
$NiCo_2S_4$/graphene	74.5/5000	1145	33.8	799.8	124
$NiCo_2S_4$/rGO	82/3000	1072	41.52	1067	125
$NiCo_2O_4$/NG/MnOOH	88/2000	525.72	7.2	548.72	126
$NiCo_2O_4$/$ZnCo_2O_4$/rGO/CNTs	84.0/6000	1128.6	50.8	800	127
$NiCo_2O_4$/Fe/rGO	78.8/12 000	2772	93.5	455	128
$NiCo_2O_4$/GO	—	530	37.8	1350	129
$NiCo_2O_4$/graphene	85/50 000	369.8	24.7	799.6	130
$NiCo_2O_4$/rGO	134/30 000	871	29.3	790.8	131
$NiCo_2O_4$/graphene	95.04/5000	1118	9.37	250	132
$NiCo_2O_4$/graphene/AC	100/1000	854	2.2 mW h cm^{-2}	45.1 mW cm^{-2}	133
$NiCo_2O_4$/rGO	92/5000	758 C g^{-1}	61	—	134
$NiCo_2O_4$/rGO/polymer	61/10 000	3160 mF cm^{-2}	0.64 mW h cm^{-2}	2.7 mW cm^{-2}	135
$Ni(OH)_2$:polyaniline/rGO	—	381.67	76.33	3.3109	136
$Ni(OH)_2$/rGO	91.4/10 000	2776	39.24	1962	137
$Ni(OH)_2$/silver/graphene/PPy	108.37/5500	237.25 C g^{-1}	43.26	750.00	138
$Ni(OH)_2$/GO/AC	80/1000	322 mF cm^{-2}	0.134 mW h cm^{-2}	33.6 mW cm^{-2}	139
$Ni(OH)_2$/Ni foam/graphene	73.1/2000	2667.2 mF cm^{-2}	143 μW h cm^{-2}	1400 μW cm^{-2}	140

194 mA h g^{-1} and the GO/PANI/$NiMoS_4$//AC supercapacitor also showed a high energy density, good cycle stability, and capacity retention. Polyaniline can provide an additional Faradaic redox reaction.[89] The selenized Ni/graphene oxide (Ni-MOF/GO) composites containing a hexa(4-carboxyl-phenoxy)-cyclotriphosphazene (NiSe/C/rGO) electrode displayed a high specific capacity of 448.9 mA h g^{-1} at 0.1 A g^{-1}. The battery-type electrode NiSe/C/rGO with improved rate capacity and cycling

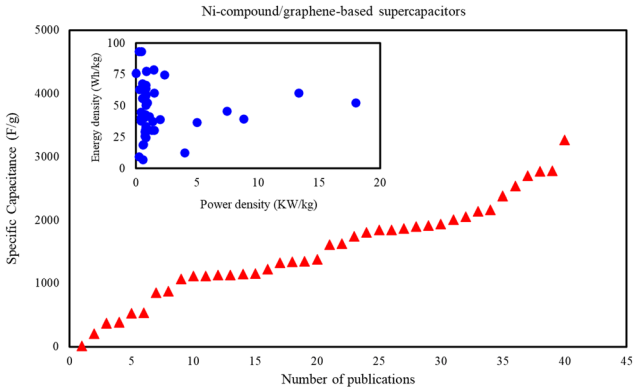

Fig. 4 Specific capacitance, power, and energy densities of Ni-materials/graphene-based supercapacitors.

stability enables an optimal SIHC with good properties.[90] $NiSe_2$ nanospheres/rGO showed an excellent specific capacity of 224.75 mA h g^{-1} at 1 A g^{-1}, and good cycling performance. Also, the $NiSe_2$/rGO//AC supercapacitor showed a high energy density and good capacity retention.[91] The Ni_3S_2/rGO electrode with 20 mg GO precursor showed the optimal areal and mass-specific capacitances. Using Ni_3S_2-20 as both the anode and cathode led to the supercapacitor with a wide potential window and high electrochemical parameters.[92] The (+) electrode of rGO/MXene/$NiCoO_2$-5 wt% has a specific capacitance of 1614 F g^{-1} at 0.5 A g^{-1} which is maintained at 1257.5 F g^{-1} when increasing the current density to 10 A g^{-1}. The supercapacitor of this electrode with rGO/MXene as the (−) electrode revealed an energy density of 45.15 W h kg^{-1}.[93] The positive electrode of thermally reduced graphene oxide (TrGO)/Ni-Foam (NF) showed a specific capacity of 52.64 mA h g^{-1} at 0.5 A g^{-1}. The supercapacitor of TRGO/NF//PAC revealed a high specific energy and outstanding stability.[94] The supercapacitor of pure graphene (−) with a Ni/graphene (+) electrode reached a specific energy of 37 W h kg^{-1} at 5 kW kg^{-1} and good reversibility.[95] Moreover, carbon-coated nano-Ni_2P (phosphides)/rGO (Ni_2P/C/rGO) was constructed and the optimal Ni_2P/C/rGO exhibited an excellent capacitance of 1338.8 F g^{-1}. It was enabled for use in supercapacitors containing an N-doped porous carbon sheet (as the opposite electrode) representing an excellent energy density of 33.4 W h kg^{-1} at 792.1 W kg^{-1}.[96] The holey graphene oxide (HGO)/nano two-dimensional Ni (Ni(BDC)-HGO30) (30 = the added HGO amount) was applied by Wang *et al.*[97] in a supercapacitor with AC (−) electrode and delivered a high outstanding property. Ni–Fe layered double hydroxide/graphene as the anode and superlong graphene nanoscrolls as the cathode were used as an anode, delivered a stable discharge capacity of 1541 mA h g^{-1}, and were employed for synthesizing a supercapacitor with the energy density of 190 kW kg^{-1}.[98] N-doped GO/$NiWO_3$/PANI nanocomposite showed an enhanced specific capacitance of 1380 F g^{-1}, and thus was found to be useful in highly stable supercapacitors.[99] The structure of LDH is prone to collapse during the redox reaction. A study assembled nitrogen-doped graphene quantum dots (N-GQD) on nickel gallium-layered double hydroxide (NiGa-LDH).[100] That study described the electrochemically interesting electrode of NiGa-LDH/N-GQD/NF was employed in the structure of a supercapacitor device containing a carbon (−) electrode. The asymmetric supercapacitor with NiGa-LDH/N-GQD/NF electrode stated a specific capacitance of 2160 F g^{-1} at 1 A g^{-1} and capacitance retention of 87.5% after 5000 cycles. The fabrication schematic of NiGa-LDH/N-GQD/NF and carbon nanosheets derived from Co-MOF electrode and the electrical properties of the asymmetric supercapacitor with electron transport of NiGa-LDH/N-GQD/NF is shown in Fig. 5. The N-GQD nanosheets can enhance the electrical conductivity, material surface polarity, and surface area with more active sites. The N-GQD nanosheets also improved the ion flow efficiency, reduced the ion transport resistance, and enhanced the redox reaction.[101,102]

2.1.1. Nickel cobalt/selenide and graphene composites. NiCo-based supercapacitors, also known as hybrid supercapacitors, combine the high energy density of batteries with the high-power density of traditional electrochemical capacitors. They are designed to provide both high energy and power capabilities for rapid energy storage and release. NiCo-based supercapacitors offer advantages such as high-power density, enabling them to deliver and absorb large amounts of energy quickly. They also have a long cycle life and good thermal stability, operating over a wide temperature range. However, their energy density is lower compared to lithium-ion batteries. NiCo-based supercapacitors are used in devices like portable electronics, electric vehicles, regenerative braking systems, and renewable energy integration, benefiting from their high-power density and rapid charge/discharge capabilities. NiCo-layered double hydroxides (NC-LDH)/rGO composites were prepared as high-performance electrodes for employment as the positive electrode in supercapacitors and AC as the negative electrode, which displayed a high electrochemical performance.[103] 3D hierarchical Ni–Co layered double hydroxides (LDH) wrapped around a porous Co_3O_4 nanocube derived from ZIF-67 were synthesized as an electrode (Ni–Co LDH/Co_3O_4 Nc). The supercapacitor constructed from this electrode and three-dimensional spongy graphene (3DSGr) showed a high energy density and superior recyclability.[104] The NiCo phosphide nano horns are formed by the Kirkendall effect for preparing the NiCo phosphide/phosphorus-doped rGO as the anode with a specific capacity of 384 F g^{-1} at 1 A g^{-1}.[105] The synthesized process of NiCo phosphides wrapped with phosphorus-doped rGO the and electrical properties of the asymmetric supercapacitor were presented in Fig. 6. The supercapacitor prepared from this electrode and AC (cathode) yields an energy density of 39.7 W h kg^{-1} at a high power density of 8.82 kW kg^{-1}. The $(Ni_{0.85}Se)_3(Co_{0.85}Se)$/rGO composite was synthesized by microwave heating followed by a solvothermal method to present the microstructure with an excellent specific capacitance of 2009 F g^{-1} at a current density of 2 A g^{-1}. The $(Ni_{0.85}Se)_3$-$(Co_{0.85}Se)$/rGO//AC supercapacitor exhibited a high energy density.[106] Ni/Co selenide/GO (NiCoSe/G) was synthesized using a water bath and selenization process and the optimized electrode (NiCoSe/G-10) exhibited a high specific capacity and an excellent cycling performance as well as a high performance of NPC//NiCoSe/G-10 supercapacitor as tabulated in Table 1.[107]

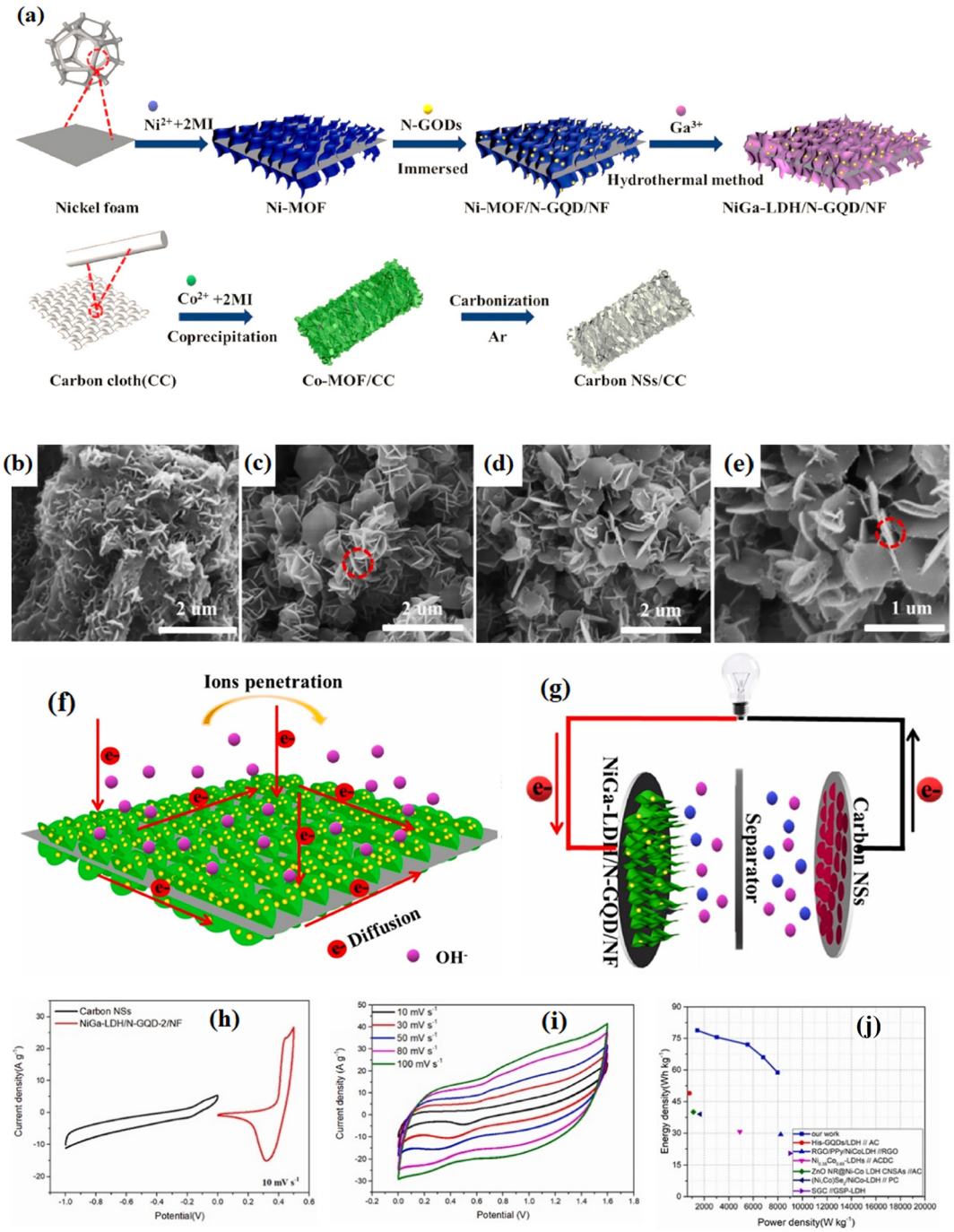

Fig. 5 (a) The fabrication of NiGa-LDH/N-GQD/NF and carbon nanosheets derived from Co-MOF electrode. The SEM images of (b) Ni-MOF/NF, (c) NiGa-LDH/NF, and (d) and (e) NiGa-LDH/N-GQD/NF. (f) A schematic of the electron transport of NiGa-LDH/N-GQD/NF. (g) The assembly diagram of NiGa-LDH/N-GQD-2/NF//Carbon NSs. (h) The CV curves of NiGa-LDH/N-GQD-2/NF and carbon NSs at 10 mV s^{-1}. (i) The CV graphs of an asymmetric supercapacitor at different scan rates. (j) A Ragone plot.[100]

Ni–Co sulfide/crystalline MnS/rGO cathodes have long-term cyclic stability and a high specific capacity of 1248 C g^{-1} at 2 A g^{-1} while ultra-small Fe_2O_3 nanodots/rGO anode showed a specific capacity of 734.2 C g^{-1} at 2 A g^{-1}. The corresponding supercapacitor showed a high specific energy of 42.0 W h kg^{-1}.[108] A supercapacitor based on 3D carbon microtubes and a vertical graphene nanosheet electrode (+) with AC electrode (−) revealed high power and energy densities.[109] The Ni–Co LDH/graphene supercapacitor showed 87.1% capacity at a high rate, whereas only 50.5% was retained for Ni–Co LDH.[110] The NiCoP/rGO-NF electrode (prepared using a hydrothermal method and low-temperature phosphating method) has a specific capacitance of 2137.8 F g^{-1} (at 1 A g^{-1} current density). The NiCoP/rGO-NF//AC supercapacitor

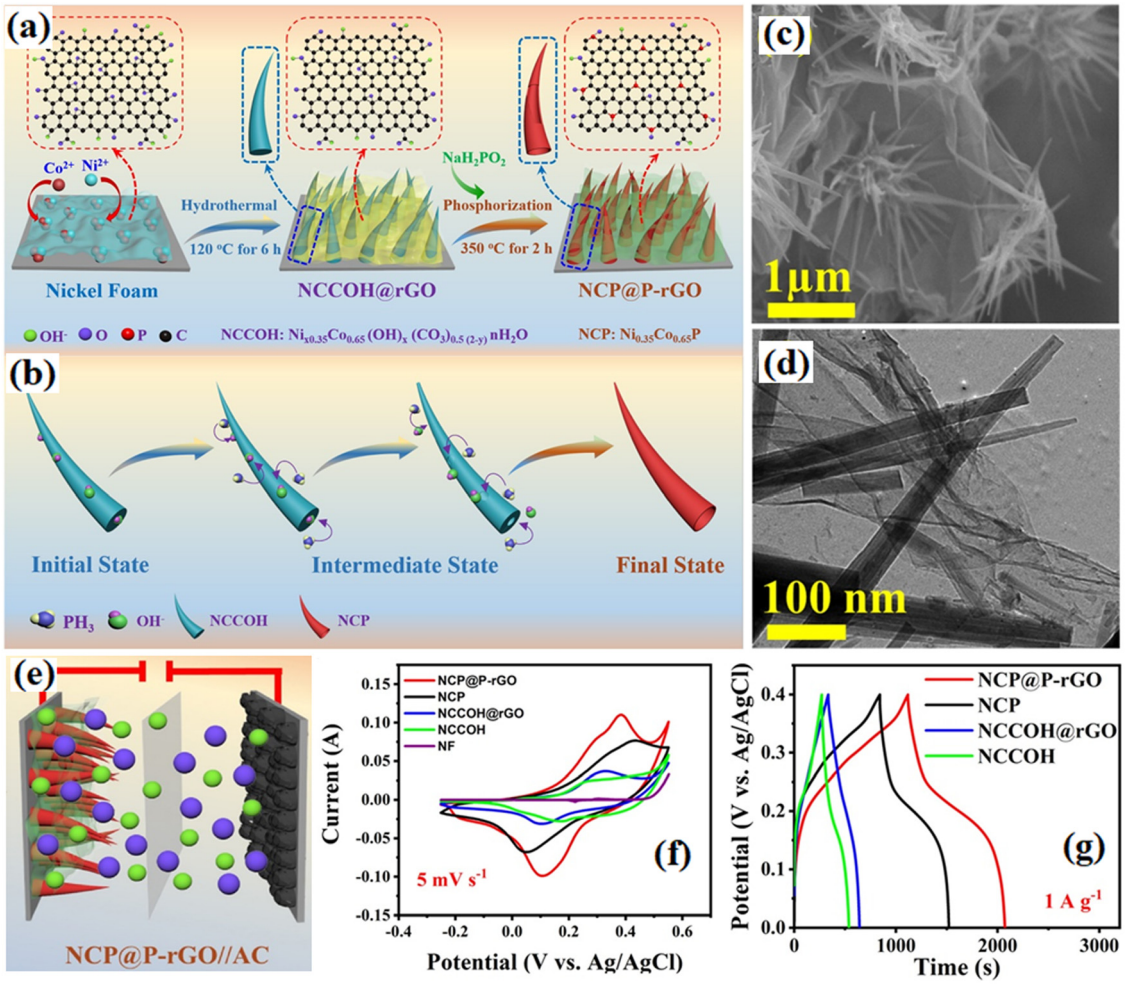

Fig. 6 (a) Synthesis of NiCo phosphides wrapped with phosphorus-doped rGO and (b) ion-exchange reaction and morphology transition mechanism of NCP@P-rGO. (C) SEM image of NCCOH@rGO. (d) TEM image of NCCOH@rGO. (e) Schematic of the supercapacitor. (f) Comparison of CV curves at 5 mV s^{-1}. (g) Comparison of GCD curves at 1 A g^{-1}.[105]

exhibited novel electrochemical traits.[111] The NiCo-LDH/N-doped graphene hydrogel (N-GH)/Nickel foam composites were prepared using a simple one-pot hydrothermal method. The NiCo-LDH/N-GH/NF//GH/CNT supercapacitor showed novel electrochemical behavior as reported in Table 1.[112] rGO/MXene/Fe_2O_3 (−) and rGO/MXene/NiCo-P (+) have an interconnected nanostructure with specific surface areas at 17.1 and 131.9 m^2 g^{-1}. An asymmetric supercapacitor showed a maximum energy density of 29.46 W h kg^{-1} at a power density of 700.34 W kg^{-1}.[113] A Hausmannite/sulfur rGO (MO/rGO-S)/Co–Ni layered double hydroxide (MO/rGO-S-50/CN) composite and the device consisting of MO/rGO-S-50/CN (+) and AC (−) delivered excellent results for using in a high specific energy supercapacitor.[114] NiCo-LDH hollow micro-tunnels strongly coupled with a higher-Fermi-level graphene quantum dots (GQDs) (GQDs/LDH-2) electrode yield an excellent capacitance of 1628 F g^{-1} at 1 A g^{-1} that when coupled with an rGO electrode (−) showed a 46 W h kg^{-1} energy density.[115] MWCNT/GO nanoribbon/Graphitic carbon nitride NNi-colayered double hydroxide/Ni foam was prepared and exhibited high specific capacitance and exceptional performance. Its supercapacitor with AC delivers a high capacitance and long cycle life.[116] The Ni–Co layered double hydroxide/rGO fibers (NCLDH/rGOFs) exhibited an outstanding area-specific capacitance of 2020 mF cm^{-2} at 5 mA cm^{-2} in a three-electrode system. Using NCLDH/rGOFs and FeOOH/rGOFs electrodes in the supercapacitor structure led to excellent properties.[117] Nickel selenide (NiSe) is used as an electrode in hybrid supercapacitors, although it is limited by poor conductivity and sluggish ion kinetics. The electrochemical performance of NiSe is improved by the addition of rGO, which can be attributed to the raised interfacial interaction and enhanced access to the active sites. Khaladkar *et al.*[118] fabricated an asymmetric supercapacitor with NiSe/rGO(+)//AC (−) electrodes and found an energy density of 49.6 W h kg^{-1} at 748.37 W kg^{-1} with a capacitance retention of 83.3% after 5000 cycles. They mentioned the possible chemical reaction processes to form NiSe as follows:[118]

$$3Se + 6OH^- \rightarrow 2Se^{2-} + SeO_3^{2-} + 3H_2O \quad (1)$$

$$Ni^{2+} + Se^{2-} \rightarrow NiSe \quad (2)$$

The Se in an alkaline atmosphere becomes Se^{2-} and SeO_3^{2-} and Ni^{2+} ions interacting with Se^{2-} create NiSe. The defects on the rGO matrix act as nucleation centers and help the growth of NiSe structures on rGO. In another study,[119] the NiSe nanoparticles on graphitic carbon nitride (g-C_3N_4) nanosheets were coated and the asymmetric supercapacitor with NiSe/g-C_3N_4//AC electrodes showed an energy density of 52.5 W h kg^{-1} at 1488 W kg^{-1} with a capacitance retention of 84.9% after 8000 cycles. This study reported the NiSe/g-C_3N_4 nanocomposite was created using the hydrothermal method and the obtained g-C_3N_4 was used during the procedure of NiSe fabrication and provided several active sites during the reaction. The reaction mechanism can be obtained from:

$$Ni(CH_3CO_2)_2{\cdot}4H_2O \rightarrow Ni^{2+} + 2(CH_3CO_2)^- + 4H_2O \quad (3)$$

$$2Ni^{2+} + 6N_2H_4 + 4OH^- \rightarrow 2[Ni(N_2H_4)_3]^{2+} + 4OH^- \quad (4)$$

$$3Se + 6OH^- \rightarrow 2Se^{2-} + SeO_3^{2-} + 3H_2O \quad (5)$$

$$[Ni(N_2H_4)_3]^{2+} + Se^{2-} \rightarrow NiSe + 3N_2H_4 \quad (6)$$

The surface charge distribution of g-C_3N_4 promotes the attachment of nanoparticles on its surface. In the reaction mechanism nickel acetate is dissociated into ions in the solution (eqn (3)). The hydrazine hydrate helps in the reduction of Ni^{2+} and dissolves Se powder in DI water (eqn (4)). After dissolution the Se under highly basic pH conditions forms Se^{2-} ions (eqn (5)). Then, the nickel complex and the Se^{2-} react together to form NiSe as a final product (eqn (6)).

2.1.2. Ternary nickel cobalt sulfide/oxides and graphene composites. Nickel and cobalt sulfides such as $NiCo_2S_4$ have emerged as exceptionally effective electrode materials for supercapacitors.[120–125] Their selection stems from a combination of advantageous characteristics, including abundant availability of raw materials, remarkable electrochemical reactivity, superior electrical conductivity, weakened metal–sulfur bonds, and enhanced thermal stability. The growth of $NiCo_2S_4$ on the g-C_3N_4/rGO heterostructure as an electrode led to the high specific capacitance of 1938 F g^{-1} at a current density of 2 A g^{-1}.[120] $NiCo_2S_4$-β-cyclodextrin graphene composite has been used as an electrode with good characteristics due to the increase in the binding force between $NiCo_2S_4$ nanoparticles and substrates.[121] The supercapacitor based on the $NiCo_2S_4$/Ni–Mo electrode exhibited a specific capacitance of 1346 F g^{-1}.[122]

The composite of CoNi Hydroxide/$NiCo_2S_4$/rGO was synthesized by Guo *et al.*[123] and showed attractive traits for the prepared supercapacitor of CoNi-LDH/$NiCo_2S_4$/rGO//AC. The cathode electrode of $NiCo_2S_4$/N, S co-doped graphene used in the supercapacitor device consisting of the graphene anode, demonstrated an outstanding energy density of 33.8 W h kg^{-1} and other characteristics.[124] Abdel-Salam *et al.*[125] employed the $NiCo_2S_4$/rGO nanocomposite with outstanding electrochemical behavior in the hybrid supercapacitor of $NiCo_2S_4$/rGO(+)//AC (−) with good electrochemical traits. Nickel cobaltite ($NiCo_2O_4$) has garnered attention as a promising energy storage material for electrochemical supercapacitors. It belongs to a new class of materials with favorable properties for energy storage applications. $NiCo_2O_4$ exhibits impressive electrochemical performance, including high specific capacitance, cycling stability, and rapid charge/discharge rates, enabling efficient energy storage and delivery. The abundance and cost-effectiveness of its constituents, nickel, and cobalt, make $NiCo_2O_4$ attractive for large-scale production. The combination of nickel and cobalt in $NiCo_2O_4$ synergistically enhances its electrochemical performance, leading to improved capacitance, conductivity, and stability, thereby advancing supercapacitor capabilities. $NiCo_2O_4$ holds promise for addressing energy storage challenges and plays a crucial role in advancing supercapacitor technology. The nanocomposite of graphene/$NiCo_2O_4$/MnOOH prepared by Yadav *et al.*,[126] showed remarkable capacitive behavior for use in a novel coin cell supercapacitor device. $NiCo_2O_4$/$ZnCo_2O_4$/graphene/carbon nanotubes with significant electrochemical properties were combined with AC electrodes for preparing supercapacitors with good energy and power densities.[127] That study presented a hybrid supercapacitor fabricated based on the NZ@GC and activated carbon electrodes, with an energy density of 50.8 W h kg^{-1} at a power density of 800 W kg^{-1}. The fabrication process of $NiCo_2O_4$/$ZnCo_2O_4$@rGO/CNTs and the electrical properties of the hybrid supercapacitor are presented in Fig. 7.

An asymmetric supercapacitor based on the Fe-doped $NiCo_2O_4$/rGO hybrid (with highly electrochemically properties) delivered superb characteristics.[128] This electrode was elaborated in hydrothermal and ultrasonic ways. An asymmetric supercapacitor device fabricated from GO/$NiCo_2O_4$/nano petals and in 1 M TEABF4 acetonitrile organic electrolyte.[129] Nano-Ni cobaltate ($NiCo_2O_4$)/crumpled graphene microspheres (CGM) due to the porous spherical architecture and good dispersion displayed ideal electrochemical properties in the aqueous supercapacitor with a negative electrode of N-doped CGM (N-CGM).[130] $NiCo_2O_4$/rGO composite with a hierarchical structure was fabricated using a facile one-step ultrasonic spray on Ni foam and directly used for supercapacitors in aqueous KOH electrolyte. Besides, the assembled $NiCo_2O_4$/rGO//AC supercapacitor displayed a maximum energy density of 29.3 W h kg^{-1} at 790.8 W kg^{-1}.[131] The obtained $NiCo_2O_4$/graphene electrode manifests a high specific capacitance as well as good steady electrochemical performances of the assembled supercapacitor under different tortuosity.[132]

The porous graphene/wood-derived carbon (GWC) aerogels were fabricated by chemical reduction of GO/wood hydrogels.[133] An activated GWC anode was prepared by activating GWC using $ZnCl_2$ while the cathode was synthesized by the growth of $NiCo_2O_4$ in the channels of GWC for use in a novel supercapacitor (with an areal capacitance of 7116 mF cm^{-2} at 1 mA cm^{-2}). Nanoribbon-like $NiCo_2O_4$/rGO nanocomposites were prepared using an oxalate-assisted hydrothermal method with various rGO contents (10, 20, and 30 wt%).[134] The $NiCo_2O_4$–30 wt% rGO//AC capacitor showed a high electrochemical characteristic. $NiCo_2O_4$/rGO nanosheets were assembled with the cement of KOH/polyacrylic acid, LiOTf/PAA, KOH/polyethylene oxide, and LiOTf/PEO into four structural

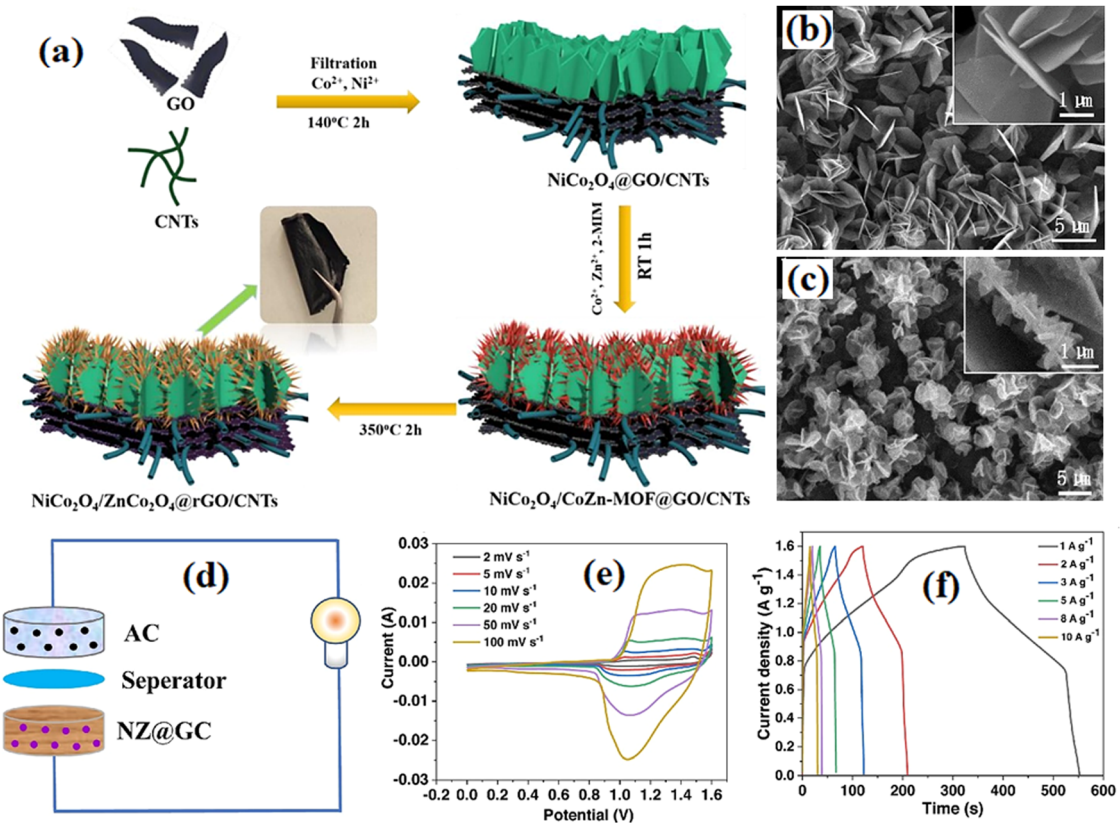

Fig. 7 (a) Fabrication process of $NiCo_2O_4/ZnCo_2O_4$@rGO/CNTs. (b) SEM image of $NiCo_2O_4$@GO/CNTs. (c) SEM image of $NiCo_2O_4/ZnCo_2O_4$@rGO/CNTs film. (d) Assembly illustration of the NZ@GC//AC hybrid supercapacitor. (e) CV and (f) GCD curves of the supercapacitor.[127]

supercapacitors.[135] The (13%) $NiCo_2O_4$/rGO electrode presents the best areal capacitance. The corresponding supercapacitors showed superior electrochemical performances, *e.g.*, areal capacitances of 330.4 mF cm^{-2}.

2.1.3. Nickel hydroxide anchored graphene. Nickel hydroxide ($Ni(OH)_2$) is highly regarded as a cathode material for supercapacitors due to its superior electrochemical activity, well-understood reaction mechanism, and cost-effectiveness. Its excellent electrochemical activity facilitates efficient charge transfer, enabling effective energy storage and release. A clear understanding of its reaction mechanism aids in optimizing supercapacitor system design for enhanced performance. Additionally, its affordability compared to other electrode materials makes it economically viable for large-scale production and widespread adoption of supercapacitor technology. $Ni(OH)_2$ has emerged as a promising choice for supercapacitor cathodes. The enhanced electrochemical results have been obtained in $Ni(OH)_2$:polyaniline/rGO/acetic acid composites using 0.4 M CH_3SO_3H as the supporting electrolyte for 0.4 M H_2SO_4 as tabulated in ref. 136. The specific capacitance of the $Ni(OH)_2$/rGO electrode was found to be remarkable and its combination with active carbon led to a supercapacitor with a high energy density.[137] A supercapacitor based on the Ag/GN/polypyrrole–$Ni(OH)_2$//AC electrodes showed a specific capacity of 237.25 C g^{-1} 1 M potassium hydroxide (KOH) solution with the observable specific capacity used in the supercapattery containing AC as a (−) electrode displaying an eminent energy density of 43.26 W h kg^{-1}.[138] This particular configuration yielded an outstanding energy density of 43.26 W h kg^{-1}, accompanied by a corresponding power density of 750 W kg^{-1}, achieved at a current density of 1.0 A g^{-1}. Moreover, that paper exhibited the cyclic stability of the supercapattery exceptional performance with a high cyclic stability of 108.37% even after enduring 5500 cycles. Fig. 8 shows the electrical properties of the Ag/GN/PPy–$Ni(OH)_2$//AC supercapacitor. The nanocomposite of $Ni(OH)_2$ nanoplates/highly-oxidized GO (HGO) was employed by Wu *et al.*[139] in a $Ni(OH)_2$/HGO//AC supercapacitor showing outstanding electrochemical properties. The electrode prepared by applying a constant potential to the Ni fiber in the alkaline solution containing GO was used in the supercapacitor of $Ni(OH)_2$/Ni foam//AC/Ni foam and showed a high specific capacitance of 543.6 mF cm^{-2}.[140] Pseudocapacitive materials are significant to the development of energy storage devices despite usually suffering from poor conductivity. A study showed the specific capacitance of $Ni(OH)_2$/GO electrode was 4.3 times higher than that of the pure $Ni(OH)_2$.[141] That study displayed the asymmetric supercapacitor with $Ni(OH)_2$/HGO//AC electrodes exhibited an energy density of 0.134 mW h cm^{-2} and 33.6 mW cm^{-2}. Also, the electrochemical performances of $Ni(OH)_2$, $Ni(OH)_2$/GO, and $Ni(OH)_2$/HGO electrodes are evaluated with 6 M KOH as the electrolyte

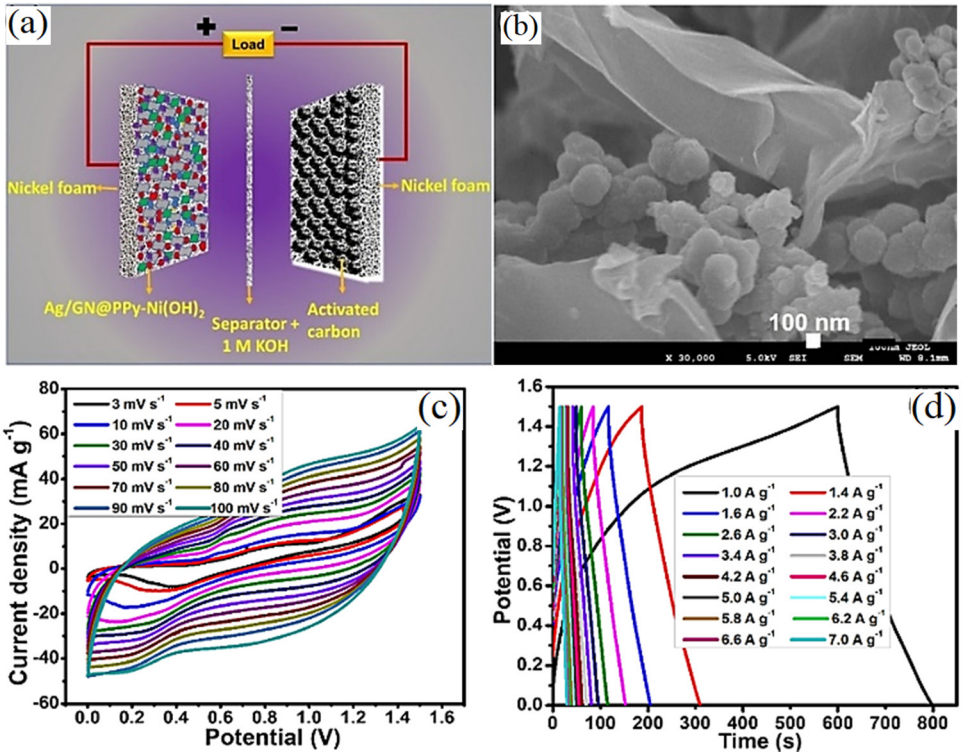

Fig. 8 (a) Schematic of supercapattery structure. (b) SEM image. (c) *C*–*V* curves. (d) Discharge curves of the Ag/GN/PPy–Ni(OH)$_2$//AC supercapattery.[138]

and observed a typical pseudocapacitive nature with the following reaction of:[142]

$$Ni(OH)_2 + OH^- \leftrightarrow NiOOH + H_2O + e^- \quad (7)$$

Lai *et al.*[143] prepared an asymmetric supercapacitor with rGO/Ni(OH)$_2$ electrode, in which rGO has some oxygen-containing functional groups that supply more sites for Ni(OH)$_2$. They achieved an energy density, power density, and specific capacitance of 1670.4 F g^{-1}, 54.1 W h kg^{-1}, and 1 kW kg^{-1} respectively, and also reported the good pseudocapacitance of Ni(OH)$_2$ is due to its rapid reversible redox reaction on the surface (eqn (7)).

2.2. Carbon nanotube-based nickel composites

Yousefipour *et al.*[144] prepared MWCNTs/NiMoO$_4$ using blending and ball-milling and it delivered outstanding supercapacitive properties because of its fast kinetics, outstanding conductivity, good surface area, and many active sites. The CNT incorporation into NiMn sulfide (NiMnS) led to the NiMnS/CNTs composites and significantly improved the storage capacity. The supercapattery was designed using NiMnS$_{75}$/CNTs$_{25}$ as the anode and an AC cathode with an outstanding specific capacity.[145] A flexible FSC was prepared based on carbon fiber/multi-layer alternating Ni–Al layered double hydroxide/mono-dispersed CNTs ([Ni–Al LDH-*x*/CNTs-*y*]/CF) as the (+) electrode, and tremella-derived AC/CF as the (−) electrode. This structure benefits from mechanical stress release, effective ion diffusion, rapid electron transfer, and high-quality loading resulting in the meaningful characteristics.[146] The highly redox-active octamethyl-substituted Ni(II)phthalocyanine (NiMe$_2$Pc)/CNTs-COOH dendritic nanocomposite provides rapid electron/electrolyte ion-transport pathways and represents excellent structural stability, resulting in highly-impressive cycling stability and capacity activity. The optimized weight ratio of NiMe$_2$Pc : CNTs-COOH (6 : 10) showed the highest specific capacitance of 330.5 F g^{-1} at 0.25 A g^{-1}. The SC device containing this electrode showed excellent performance with a maximum energy density of 22.8 W h kg^{-1} and outstanding cycling stability (111.6% retained after 35 000 cycles).[147] Also, between the Ni phosphate (NiP)/MWCNTs (10, 30, and 50 wt%) samples, NiP$_{50}$CNT$_{50}$ revealed a better specific capacity of 845 C g^{-1} at 0.6 A g^{-1} and better supercapacitor performance with a specific capacity of 400 C g^{-1} at 0.4 A g^{-1}.[148] In another study, the MWCNTs/Ni–Mn–S were prepared and achieved excellent properties. The as-prepared MWCNTs/Ni–Mn–S (3 : 2) exhibit a specific capacitance of 1041 mA h g^{-1} at 1 A g^{-1} and good cycling stability. The MWCNT/Ni–Mn–S (3 : 2)//AC supercapacitor also showed outstanding cycling stability of 93.3%/20 000.[149]

2.2.1. Carbon nanotubes decorated with nickel cobalt. A high-performance supercapacitor can be created by integrating Ni materials/CNTs. This combination enhances the energy storage capacity and facilitates rapid charge transfer. The supercapacitor exploits the reversible redox reactions of the Ni materials and the conductivity of CNTs to store and release charge efficiently. Through careful optimization of synthesis methods, electrode designs, and electrolyte selection,

a powerful Ni-material/CNT-based supercapacitor can be developed. Su *et al.*[150] prepared P-doped Ni–Co sulfides (P-NCS)/C/CNT composites by gas-solid phosphorization that revealed high specific capacity (932.0 C g^{-1} at 1 A g^{-1}) and remarkable rate capability and also were used in flexible supercapacitors containing AC (as an opposite electrode), which exhibited high energy and power densities. Alternatively, the composites of NiCo-P (phosphate)/CNTs/lightweight carbonized wood were synthesized by chemical vapor deposition and electrodeposition showing a promising notable capacitance retention and rate areal capacitance. Also, its usage in supercapacitors composed of self-activated carbonized wood (SCW) electrodes as a cathode delivered outstanding traits.[151] CNTs/Ni–Co sulfide composites exhibited the synergy between the components. It was used by Huang *et al.*[152] as a positive electrode with a high specific capacity of 734 C g^{-1} in the supercapacitor of CNTs/Ni–Co–S-3//AC HSC with an energy density of 42.15 W h kg^{-1} and long-term stability. Another study reported an asymmetric fiber-shaped FSC made of carbon fiber, Ni–Co layered double hydroxide, and mono-dispersed CNTs (Ni–Co LDH-*x*/CNTs-*y*/CF) as the positive electrode and tremella-derived activated carbon/CF (TDC-z/CF) as the negative electrode. The prepend FSC achieved a high energy density of 26.20 W h kg^{-1} and a superior cycling stability of 112.5% over 5000 cycles.[153] A supercapacitor based on the NiCo-phosphide/NiCo-layered double oxide-CNTs (NCP/LDO-CNTs) composite showed a specific capacity of 901.2 mA h g^{-1}.[154] The porous NiCo nanoparticles/N-doped CNTs/carbon cloth/NiCo hydroxide was prepared so that NiCo@NCNTs can act as a good conductor and structural scaffold to grow NiCo-LDH nanosheets. It displayed novel electrochemical traits as a (+) electrode. Also, its usage in a supercapacitor with a $Co(OH)_2$/NiCo@NCNTs/CC negative electrode led to 52.8 W h kg^{-1} of energy density.[155] Yuan *et al.*[156] investigated a supercapacitor based on the Ni–Co–Se/C-CNTs electrode and achieved a specific capacitance of 1108.2 F g^{-1}. They mentioned the power and energy densities of Ni–Co–Se/C-CNTs//AC supercapacitors were 38.2 W h kg^{-1} and 1602.1 W kg^{-1}, respectively. Fig. 9 shows the electrical properties of the Ni–Co–Se/C-CNTs//AC supercapacitors.

2.2.2. Ternary nickel cobalt sulfide/oxides and carbon nanotube composites. The electrochemical properties of supercapacitors on the basis of Ni materials and CNTs composite electrodes are reported in Table 2[144–163] The nanocomposite CNTs/$NiCo_2S_4$ showed remarkable capacitive properties. In the structure of the asymmetric supercapacitor, it exhibited energy and power densities of 43.3 W h kg^{-1} and 800 W kg^{-1}. The exceptional electrochemical capacity is attributed to the enhanced conductivity, refined grains, and structural features.[157] NiCo sulfide ($NiCo_2S_4$) was prepared with the help of a shadow mask printing method on a flexible PET substrate using homemade ink comprised of PTFEm, CNTs, $NiCo_2S_4$, carbon nanotubes, and terpineol. The $NiCo_2S_4$ electrode revealed a high specific capacitance of 1401 F g^{-1} while the

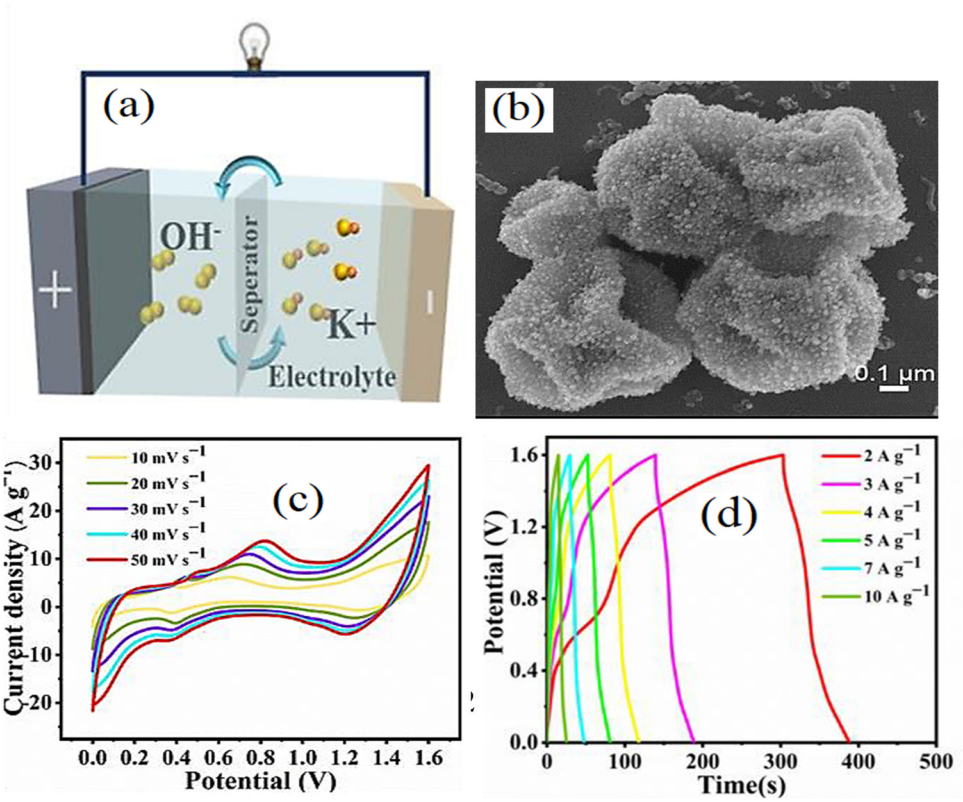

Fig. 9 (a) Schematic of the supercapacitor structure. (b) SEM image. (c) *C–V* curves. (d) Discharge curves of the Ni–Co–Se/C-CNTs//AC supercapacitor.[156]

Table 2 The electrochemical results collected from various studies done on Ni/CNT nanocomposites

Material	Capacitance retention (CR%/Cycle)	Specific capacitance ($F\ g^{-1}$)	Energy density ($W\ h\ kg^{-1}$)	Power density ($W\ kg^{-1}$)	Ref.
$NiMoO_4$/CNTs	86.8/2000	727.2	40.9	918.5	144
$NiMnS_{75}$/CNTs	—	1188 C g^{-1}	9	1600.8	145
Ni/CNTs	124.8/5000	1800	35.6	7531.90	146
$NiMe_2Pc$/CNTs	95.4/35 000	330.5	52.1	—	147
Ni phosphate/CNTs	—	845 C g^{-1}	94.4	340	148
Ni–Mn/CNTs	83.3/10 000	1041 mA h g^{-1}	25.33	829	149
Ni–Co sulfides/CNTs	—	932.0 C g^{-1}	34.875	375	150
Ni–Co phosphate/CNTs	92.4/10 000	11.2 F cm^{-2}	12.1	39.5	151
Ni–Co–S-3/CNTs/AC	88.46/10 000	734 C g^{-1}	42.15	852	152
Ni–Co/CNTs	112.5/5000	—	26.20	7569.23	153
Ni–Co phosphide/CNTs	117.4/4500	1888	21.3	748.5	154
Ni–Co/CNTs	100/8000	1898 mF cm^{-2}	52.8	—	155
Ni–Co–Se/C-CNTs	96.4/5000	1108.2	38.2	1602.1	156
$NiCo_2S_4$/CNTs	83.5/5000	890 C g^{-1}	43.3	800	157
$NiCo_2S_4$/PET/CNTs/PTFE	90/3000	13.6 mF cm^{-2}	2.1 μW h cm^{-2}	0.189 mW cm^{-2}	158
$NiCo_2S_4$/CNTs		443 F cm^{-3}	11.7	1320	159
$NiCo_2S_4$/CNT	96.08/10 000	2498.12	76.47	201.01	160
$NiCo_2$/CNTs	76.4/2500	1311.8	27.19	750	161
$NiCoO_2$/CNTs	92/5000	1587	41.8	412	162
$NiCo_2O_4$/CNTs	82/50 000	588 mF cm^{-2}	138 μW h cm^{-2}	—	163

device delivered a value of 13.6 mF cm^{-2}.[158] A typical battery-type electrode of $NiCo_2S_4$/CNTs prepared by Yao *et al.*[159] exhibited an ultrahigh specific capacitance of 1123 F g^{-1} at 0.5 A g^{-1}, superior stability, and good energy storage ability. A supercapacitor constructed from this electrode (cathode) and treated carbon cloth (anode) showed a high energy density of 11.7 W h kg^{-1} with good cycling stability. The porous $NiCo_2S_4$ nanosheet/conductive carboxylated CNTs (CNTs-h-COOH) composite was synthesized and the deposition potential and time played important roles in influencing the morphology and electrochemical performance of the composite. This electrode and a supercapacitor contained commercial AC (as the anode) resulting in outstanding specific capacity and energy density.[160] In the case of N-doped CNTs/NiCo layered double hydroxides(N-CNTs/NiCo-LDH), the samples of N-CNTs/$Ni1Co_2$-LDH had the best electrochemical performance. Also, the N-CNTs/$Ni1Co_2$-LDH(+)//AC(−) supercapacitor had a high energy density of 27.19 W h kg^{-1} at 750 W kg^{-1}.[161] The bimetal oxide ($NiCoO_2$)/CNTs with a novel mesoporous grape-like structure were prepared that due to the synergistic effect, showed impressive properties. The supercapacitor ($NiCoO_2$/CNTs//AC) exhibited an outstanding cycling property with 92% maintained after 5000 cycles.[162] A kapok-derived proper-curved quasi-2D carbon tile (CT)/SWNTs/$NiCo_2O_4$ electrode was constructed *via* a scalable and controllable extrusion-based 3D printing strategy. A corresponding supercapacitor delivered a high specific capacitance (588 mF cm^{-2}) and superior capacity even at large electrode thickness.[163] Transition metal sulfides are promising electrodes due to the high conductivity and lower electronegativity of sulfur. Sammed *et al.*[164] fabricated a composite of carbon nanocoils/nickel foam (CNCs/NF) substrate that was decorated with nickel cobalt sulfide ($NiCoS_x$) nanosheets and CNTs. They elucidated that the specific capacitance of the CNTs/$NiCoS_x$/CNCs/NF electrode was 3184 F g^{-1} with a capacitance retention of 97.2% after 3000 cycles. The redox reactions of $NiCo_2O_4$ and $NiCo_2S_4$ in the alkaline electrolyte can be obtained from:[165]

$$NiCo_2O_4 + OH^- + H_2O \rightarrow NiOOH + 2CoOOH + 2e^- \quad (8)$$

$$CoOOH + 2OH^- \rightarrow NiSOH + 2CoSOH + 2e^- \quad (9)$$

$$NiCo_2S_4 + 2OH^- \rightarrow NiSOH + 2CoSOH + 2e^- \quad (10)$$

$$CoSOH + OH^- \rightarrow CoSO + H_2O + e^- \quad (11)$$

2.3. Dispersion of Ni materials in porous carbon

Table 3[166–181] demonstrates that supercapacitor electrodes based on a combination of Ni materials and porous carbon materials are widely used to enhance energy storage applications. Porous carbon, such as activated carbon or carbon nanotubes, provides a large surface area for electrochemical reactions and ion adsorption. Ni materials offer excellent electrical conductivity and redox properties. The performance of the supercapacitor is evaluated using tests like cyclic voltammetry and galvanostatic charge–discharge cycling. Panicker *et al.*[166] synthesized porous carbon self-repairing g-C_3N_4 (pCCN)/$NiCo_2S_4$ for supercapacitor electrodes that showed a remarkably high specific capacitance. The constructed pCRNCS//AC exhibited a remarkable capacitance retention of 93.6% and 6000 cycles and an energy density of 66 W h kg^{-1}. The porous and three-dimensional AC (BPC) was prepared by calcining and etching the Platanus fluff. The $NiCo_2S_4$/BPC electrode displayed a better characteristic than that of the pure $NiCo_2S_4$. The supercapacitor of $NiCo_2S_4$/BPC displayed a high energy density and superior cycling stability.[167] N-doped lignite-based porous carbon (NPC)/$CoNi_2S_4$ ($CoNi_2S_4$/NPC) as the electrode material displayed excellent specific capacitance and good cycle performance. The supercapacitor of $CoNi_2S_4$/NPC (cathode)//AC (anode)

Table 3 The electrochemical results collected from various studies done on Ni/porous carbon nanocomposites

Electrode material	Capacitance retention (CR%/cycle)	Specific capacitance ($F\ g^{-1}$)	Energy density ($W\ h\ kg^{-1}$)	Power density ($W\ kg^{-1}$)	Ref.
$NiCo_2S_4$/porous carbon/g-C_3N_4/rGO	93.6/6000	211	66	751	166
$NiCo_2S_4$/porous carbon	—	175	38.5	738.1	167
$CoNi_2S_4$/porous carbon	82.42/5000	1534.24	48.58	400	168
$NiCo_2O_4$/porous carbon	—	1002.2	32.7	160.2	169
$NiCo_2O_4$/porous carbon	78/—	1474.2	53	—	170
$NiCo_2O_4$/porous carbon	80/—	1730	56.1	349	171
$NiFe_2O_4$/porous carbon	90.2/10 000	2894	135.2	10 040	172
$NiMoO_4$/porous carbon	90.7/3000	1600	55.33	999.89	173
Ni–Co/porous carbon/GO	92.6/3000	407.5	12.32	499.99	174
Ni–Co/porous carbon	90.76/3000	1504	33.33	—	175
Ni–Co/porous carbon	60/—	250	78	—	176
Ni–Co/porous carbon	87.87/10 000	415	35.6	500.1	177
Ni–sulfide/porous carbon	95.7/10 000	360	19.65	450	178
Ni–cobalt/porous carbon	75.9/4000	2390	52.47	375	179
Ni-MXene/porous carbon	81.7/30 000	152.6	47.6	375	180
$Ni(OH)_2$-MXene/porous carbon	90/5000	—	29.3	800	181

demonstrated an energy density of 48.58 W h kg^{-1} and power density of 400 W kg^{-1}, with a capacitance retention of 82.42% after 5000 cycles.[168] Wang *et al.*[169] synthesized the composites of $NiCo_2O_4$-4*x* nanowires (O vacancies-rich)/porous carbon (derived from discarded cigarette ash) named Ov-NCO/PC-Y resulting in a superior specific capacitance of 1002.2 F g^{-1}. Moreover, the Ov-NCO/PC-0.1//AC-based supercapacitor delivered an elevated energy density. N-doped porous carbon nanofiber/$NiCo_2O_4$ nanoneedles ($NiCo_2O_4$/NPCNFs) electrode materials resulted in a competitive specific capacitance as well as good rate performance (78.0% at 10 A g^{-1}). Also, the corresponding supercapacitors exhibited a high energy density.[170]

A supercapacitor based on the porous carbon-$NiCo_2O_4$ electrode was reported in ref. 171. This report determined the specific capacitance of the supercapacitor to be 1730 F g^{-1} with energy and power densities of 56.1 W h kg^{-1} and 349 W kg^{-1} respectively. Fig. 10 shows the electrical properties of the supercapacitor based on the porous carbon–$NiCo_2O_4$ electrode. Ni ferrite nanoparticle/carboxymethyl cellulose-derived porous

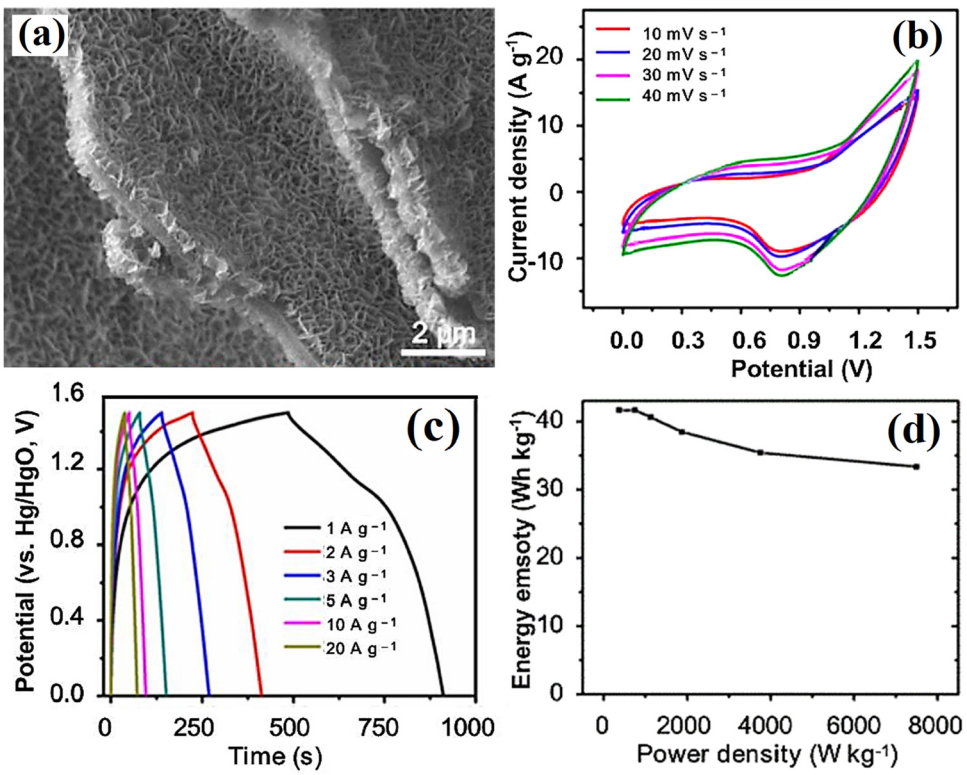

Fig. 10 (a) SEM image, (b) *C*–*V* curves, (c) discharge curves, and (d) energy and power densities of the supercapacitor based on the porous carbon–$NiCo_2O_4$ electrode.[171]

carbon ($NiFe_2O_4$/CPC) was prepared so that the best-performing sample ($NiFe_2O_4$/CPC-800) exhibited a superior capacitance. A supercapacitor with (+) electrode of $NiFe_2O_4$/CPC-800 and AC (−) electrode delivered a high characteristic.[172] Yan *et al.*[173] produced the $NiMoO_4$ (nanosheet-like)/Porous sub microfibers (HPCMFs) showing good electrochemical characteristics. A supercapacitor containing $NiMoO_4$/HPCMFs electrodes showed a high flexibility and energy and power density.

The mixture of lignin-removed poplar powder, graphene oxide, melamine, diammonium hydrogen phosphate, and nickel sulfate was carbonized and activated with KOH for preparing a porous carbon material with a pore volume of 0.93 $cm^3\ g^{-1}$ and a surface area of 1214.1 $m^2\ g^{-1}$. The prepared sample showed good performances such as outstanding power and energy densities for a supercapacitor.[174] A highly graphitized N self-doped hierarchical porous carbon aerogel (HPCA) was prepared using biomass chitosan particles as the precursor and then composited with NiCo double hydroxide (NiCo-LDH) nanosheets. A NiCo-LDH/HPCA-30 composite was designated as an optimized sample with the highest electrochemical performance.[175] The biomass lignin-derived and N-doped carbons (LPCs), *i.e.*, the activated N-doped LPCs (N-LPCs) with the porous microstructure (BET surface area: 1990.49 $m^2\ g^{-1}$) were synthesized and showed excellent electrochemical parameters. Also, as an anode, it was used in a supercapacitor combined with the cathode of NiCo double hydroxide (NiCo-LDH) and demonstrated an excellent specific capacitance.[176] The green cellulose-based N/Ni co-doped porous carbon (PC) was prepared with a high specific surface area and total pore volume and outstanding specific capacitance and excellent cycling stability. Also, the form of supercapacitor led to an energy density of 35.6 W h kg^{-1}.[177]

Ni sulfide composite with porous carbon (Ni_3S_2/HPCs) derived from coke solid waste was synthesized. The optimized Ni_3S_2/HPC-3 exhibited a high capacitance of 360 F g^{-1} and its existence in the supercapacitor structure led to a high cycle stability and energy density.[178] In another study, hydrophilic NiCo/layered double hydroxides (LDHs)/biomass waste-derived porous carbon (BC) was prepared. Due to the ultrathin thickness of LDHs, large specific surface area, low charge transfer resistance, and high wettability with electrolyte, the Ni_2Co1-LDHs/BC50 electrode revealed an ultra-high S.C. and the Ni_2Co1-LDHs/BC50//YP-80F HSC delivered a maximum specific energy of 52.47 W h kg^{-1}.[179] Nanda *et al.*[180] synthesized Ni MXene (cathode) and Euphorbia milii plant leaf-originated and N, S, P self-doped AC (EMAC-700) (anode). NiMX and EMAC-700 delivered high capacitances of 474.3 and 575.8 F g^{-1}, respectively, attributed to the pseudo nature of NiMX, the presence of heteroatoms, and the large surface area of EMAC-700. The prepared supercapacitor also showed a 152.6 F g^{-1} capacitance as well as an ultrahigh energy density of 47.6 W h kg^{-1}. Alternatively, 50MXene/50$Ni(OH)_2$ was developed as the α-$Ni(OH)_2$ petals are slid within the MXene structure for use as a cathode in combination with the biomass-derived porous carbon as the anode in the supercapacitor system. The good electrochemical performance was manifested (energy density of 29.3 W h kg^{-1}, and capacitance retention of 90% after 5000 cycles) for this supercapacitor.[181]

2.4. Ni materials//active carbon-based asymmetric supercapacitors

Active carbon, with its high surface area and porosity, finds significant application as an electrode material in supercapacitors. Its porous structure allows for efficient ion adsorption, resulting in enhanced capacitance. Active carbon electrodes enable rapid charge and discharge, making them suitable for applications requiring high power output and quick response times. They contribute to the overall energy density of supercapacitors, albeit lower than batteries, by delivering a significant amount of energy in short bursts. Active carbon exhibits excellent stability and longevity, ensuring a long cycle life and reliable performance of the supercapacitor electrodes. These electrodes have been instrumental in the development of high-performance supercapacitors used in energy storage systems, portable electronics, hybrid vehicles, and renewable energy technologies. The various supercapacitors based on the Ni materials//active carbon electrodes have been employed in electrochemical applications, and the novel results of the reported papers are tabulated in Table 4.[182–219] The utilization of active carbon in supercapacitors highlights its valuable role in improving energy storage capabilities and supporting advancements in various fields where efficient power delivery and rapid energy transfer are essential. $Ni(OH)_2$/ZIF-67-derived CoS core/carbon cloth ($Ni(OH)_2$/CoS/CC) was used in the supercapacitor of $Ni(OH)_2$/CoS/CC (cathode)//AC (anode) that revealed a remarkable energy density as well as its excellent electro-catalytic activity towards methanol oxidation.[182] La/$Ni(OH)_2$ nanosheets were prepared and the La–$Ni(OH)_2$(0.3) with 0.3 mmol of the La showed the best electrochemical traits. La–$Ni(OH)_2$(0.3)//AC delivered an energy density of 47.5 W h kg^{-1} and excellent stability of 89.3% after 2000 cycles.[183] Flower-like Zn-doped $Ni(OH)_2$/CNTs were synthesized assisted by cetyltrimethylammonium bromide (CTAB) and $NaBH_4$. This electrode showed prominent electrochemical properties and the supercapacitor of Zn doped $Ni(OH)_2$@CNTs(+)//(−)AC exhibited high electrochemical performance.[184] A 3D 2-nodal (3,8)-c tfz-d metal–organic framework (MOF 1) of {[$Co_{1.5}$(TCPB)(1.3-bomb)$_{0.5}$·(DMF)·(dioxane)$_{1.5}$]}n has been synthesized and calcined at 700 °C under a N_2 atmosphere to obtain Co/C composite (NC_1). 2D flake $Ni(OH)_2$ was coated on the surface of NC_1 to prepare $Ni(OH)_2$/NC_1 (NC_2). The specific capacitances of 866.8 F g^{-1} for the NC_2-based electrode were more than three times as much as that of the NC1-based electrode (264.5 F g^{-1}). The supercapacitor of AC (−)//(+) NC_2@NF showed an energy density of 39.7 W h kg^{-1}.[185]

The optimized pre-lithiated Ni_3Se_2 cathode (Li_2–Ni_3Se_2) was prepared and presents a high specific capacitance of 236 mA h g^{-1}as well as excellent cycling stability of 92% after 3000 cycles. It is far superior to other battery-type TMC cathodes reported in previous studies. The supercapacitor Li_2–Ni_3Se_2//AC delivered a high energy density of 77 W h kg^{-1} and high capacitance retention.[186] The hollow Ni_3S_2/Co_9S_8

Table 4 The electrochemical results collected from supercapacitors with Ni//active carbon electrodes

Electrode material	Capacitance retention (CR%/cycle)	Specific capacitance ($F\ g^{-1}$)	Energy density ($W\ h\ kg^{-1}$)	Power density ($W\ kg^{-1}$)	Ref.
$Ni(OH)_2$/CoS/CC//AC	—	561.6 mA h g^{-1}	90.8	800	182
$Ni(OH)_2$-La//AC	89.3/2000	1510.7	47.5	375	183
$Ni(OH)_2$/CNTs/Zn//AC	—	750.5 C g^{-1}	51.3	409.6	184
$Ni(OH)_2$/Co/C//AC	97.3/1000	866.8	39.7	213.1	185
Ni_3Se_2–Li_2//AC	92/3000	236 mA h g^{-1}	77	4000	186
Ni_3S_2/Co_9S_8//AC	80.8/10 000	9.79 F cm^{-2}	0.63 mW h cm^{-2}	1.66 mW cm^{-2}	187
Ni_3S_4/$MnCo_2O_4$//AC	—	904.7 C g^{-1}	50.7	405.8	188
Ni_3S_2–Co_3S_4/Ni foam//AC	92.8/2000	2825.5 mF cm^{-2}	40.9	1566.4	189
Ni-MOF/polypyrrole//AC	90.2/3000	1815.4	38.5	7001	190
Ni-MOF/C//AC	100/5000	828	23.84	849.74 W g^{-1}	191
Ni–Co-MOF//AC	82.4/7000	832.6 C g^{-1}	45.3	7160	192
NiCoS/NiMo//AC	54/—	1302.5 μAh cm^{-2}	1096.6 μW h cm^{-2}	2.8 mW cm^{-2}	193
SnNiCoS//AC	82.9/8000	18.6 F cm^{-2}	937.2 μW h cm^{-2}	4000 μW cm^{-2}	197
NiMn/$CuCo_2O_4$//AC	94.6/2500	2156.53	92.2	730	198
$NiCo_2O_4$@$NiCo_2O_4$//AC	83.6/5000	1398.73	46.46	269.77	199
Ni–Mn–S/rGO//AC	77.78/5000	2042.22	77.95	750	200
$Ni_xMn_{1-x}(OH)_2$//AC	94.4/3000	758.7	40.7	800	201
$Ni_xCo_y(OH)_2$/$Co(BO_2)_2$//AC	98/10 000	2257	56.5	800	202
Ni–Co//AC	92.5/10 000	2458.1	62.7	714.3	203
Ni–Co//AC	90.5/—	3483	34.6 mW cm^{-2}	—	204
Ni–Co–P(6)//AC	—	1384	51.2	749.8	205
Ni–Co//AC	91/5000	325.6 mA h g^{-1}	50.5	750	206
Ni–Co/NF/MnCo2O4//AC	78.7/5000	4555	21.3	160	207
Ni–Co/ZnO//AC	86.78/2000	667.3 mF cm^{-2}	0.044 mW h cm^{-2}	1.17 mW cm^{-2}	208
$NiCoZnS_x$//AC	80/10 000	1928	270 μW h cm^{-2}	80.3 mW cm^{-2}	208
NiCoP/CC//AC	99.7/10 000	1149.2 C g^{-1}	78.5	799.5	210
NiCoP//AC	90.2/10 000	1088.9 C g^{-1}	78.2	799.9	211
NiCoAl//AC	87.5/10 000	23.85 F cm^{-2}	3.29 mW h cm^{-2}	18 mW cm^{-2}	212
NiCoMn/C//AC	92.05/5000	888.3 C g^{-1}	46.5	792.5	213
$NiCo_2S_4$//AC	81/10 000	857 C g^{-1}	48.7	801	214
$NiCo_2S_4$/Co_9S_8//AC	62.8/—	1026	30	731.8	215
$NiCo_2S_4$//AC	88.9/5000	559.3 C g^{-1}	28.8	375.0	216
$NiCo_2O_4$//AC	80.9/3000	2690	52.6	1100	217
$NiCo_2O_4$–In/CF//AC	89.3/10 000	2375.1	60.2	985.5	218
$NiCo_2O_4$/MXene//AC	—	73.8	94.46	2882.0	219

(NiS/CoS) were prepared with a high active area and showed remarkable electrochemical properties. The supercapacitor of NiS/CoS(+)//AC(−) achieved a high energy density of 0.63 mW h cm^{-2}.[187] The $MnCo_2O_4$/Ni_3S_4 nanocomposite was prepared to solve the low $MnCo_2O_4$ electrical conductivity. The high performances of this electrode and its supercapacitor with active carbon were observed.[188] Co_3S_4–Ni_3S_2 on Ni foam (NF) with the assistance of a chelating agent sodium 5-sulfosalicylic (SSS) (CS_4–Ni_3S_2/F-SSS) revealed a specific capacitance of 2825.5 mF cm^{-2}. Moreover, the supercapacitor of CS_4–Ni_3S_2/F-SSS//AC/NF represents an energy density of 40.9 W h kg^{-1} with excellent durability.[189]

Ni-based metal–organic framework (Ni-MOF)/polypyrrole (PPy) had a specific capacitance of 1815.4 F g^{-1} and Ni-MOF/PPy(+)//(−)AC supercapacitors can provide capacitance retention of 90.2% after 3000 cycles, an energy density of 38.5 W h kg^{-1} and power density of 7001 W kg^{-1}.[190] Ni-metal–organic framework (MOF)/nanocarbon (NC) electrode materials were synthesized and delivered 828 F g^{-1}. The supercapacitor of Ni-MOF/NC//AC showed a capacitance retention of 100% after 5000 cycles.[191] A hydrangea-like NiCo-MOF (metal–organic framework) was well prepared revealing superior gravimetric capacity (832.6 C g^{-1} at 1 A g^{-1}). The supercapacitor of NiCo-MOF (cathode)//AC (anode) delivered a desirable energy density (45.3 W h kg^{-1}) and a favorable power density (7160.0 W kg^{-1}).[192] The NiCoS(sulfur)/NiMo-LDH electrode exhibited a very high capacitance of 1302.5 μAh cm^{-2}. The supercapacitor of the NiCoS/NiMo-LDH//AC exhibited an energy density of 1096.6 μW h cm^{-2}.[193] Tao *et al.*[194] encapsulated iron carbide nanoparticles into carbon nanofibers (Fe_3C@CNF-650), and then nickel–cobalt sulfide nanoparticles were grown on electrospun carbon nanofibers (CNF@NiCoS-650). The conductivity of carbon nanofibers facilitates Faradaic charge transport. They reported the asymmetric supercapacitor with Fe_3C@CNF-650 (−)//CNF@NiCoS-650 (+) electrodes achieved an energy density of 43.2 W h kg^{-1} at 800 W kg^{-1}. The electrochemical processes involve fast reversible redox reactions of Ni^{2+}/Ni^{3+}, Co^{2+}/Co^{3+}, and Co^{3+}/Co^{4+} reacting with OH^- anions and can be obtained from:[185–196]

$$NiS + OH^- \leftrightarrow NiSOH + e^- \quad (12)$$

$$CoS + OH^- \leftrightarrow CoSOH + e^- \quad (13)$$

$$CoSOH + OH^- \leftrightarrow CoSO + H_2O + e^- \quad (14)$$

SnNiCoS sulfide in the supercapacitors showed the best performance in that a specific capacitance of 18.6 F cm^{-2} and an energy density of 937.2 μW h cm^{-2} was achieved.[197] Zhao *et al.*[198] prepared the $CuCo_2O_4$@NiMn LDH//AC as

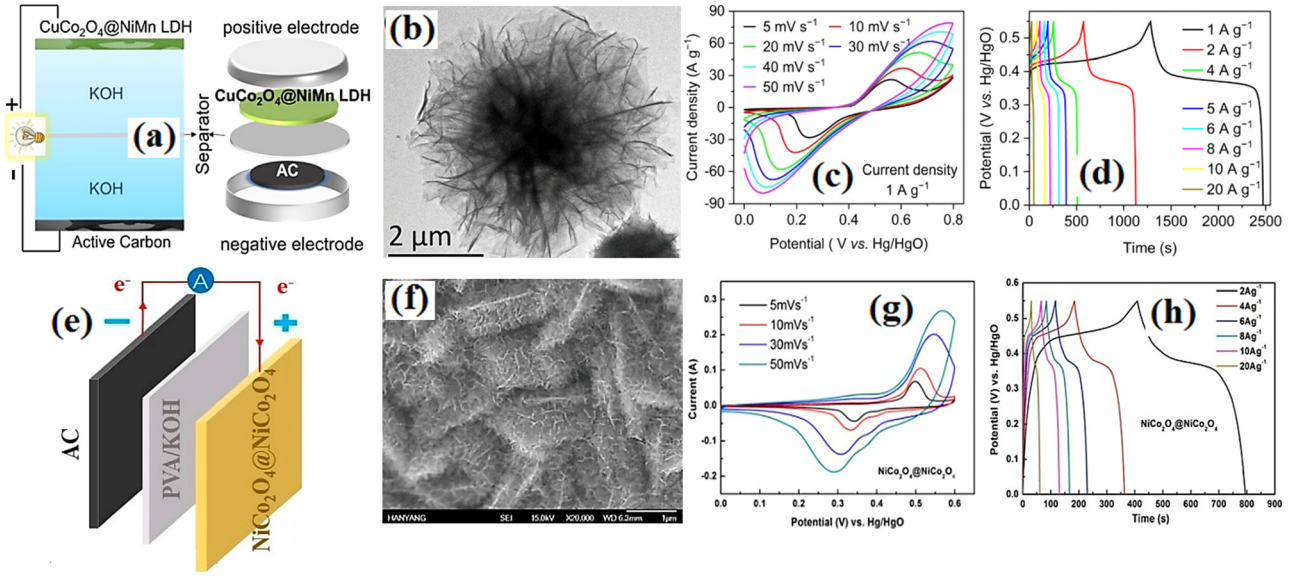

Fig. 11 (a) Graphical structure. (b) TEM image. (c) *C–V* curves. (d) Discharge curves of $CuCo_2O_4$@NiMn LDH//AC supercapacitor.[197] (e) Graphical structure. (f) SEM image. (g) *C–V* curves. (h) Discharge curves of the $NiCo_2O_4$@$NiCo_2O_4$//AC supercapacitor.[199]

supercapacitor electrodes and exhibited a specific capacity of 2156.53 F g^{-1} with a rate capability retention of 94.6% after 2500 cycles. A supercapacitor based on the $NiCo_2O_4$@$NiCo_2O_4$// AC electrodes is reported in ref. 199. That paper reported that the energy density of the supercapacitor was 46.46 W h kg^{-1} and the power density was 269.77 W kg^{-1}. Fig. 11 shows the electrical properties of the supercapacitor based on the $CuCo_2O_4$@NiMn LDH//AC and $NiCo_2O_4$@$NiCo_2O_4$//AC electrodes.

The optimized Ni–Mn–S/rGO composite revealed a superior specific capacitance of 2042.22 F g^{-1} and the supercapacitor prepared by using this electrode showed a high energy density of 77.95 W h kg^{-1} with good cycle stability.[200] The optimal composition of Ni_3/4Mn1/4$(OH)_2$ hydroxide showed a capacitance of 758.7 F g^{-1}. While the Ni_3/4Mn1/4$(OH)_2$//AC supercapacitors exhibited a high energy density of 40.7 W h kg^{-1} capacitance retention of 94.4% after 3000 cycles.[201] 2D Ni–Co hydroxide/BO_2 ($(Ni_xCo_y)(OH)_2/Co(BO_2)_2$) was prepared and the optimized electrode of $(Ni_{0.5}Co_{0.5})(OH)_2/Co(BO_2)_2$ delivered a remarkable specific capacitance of 2257 F g^{-1}. The $(Ni0.5Co0.5)(OH)_2/Co(BO_2)_2$//AC supercapacitors provided a high energy density and excellent cyclic stability.[202]

2.4.1. Nickel cobalt composite//active carbon-based asymmetric supercapacitors. The optimal honeycomb NiCo-LDH (layered double hydroxide)/carbonized polydopamine (PDA-C/NiCo-LDH) exhibited a high capacitance along with superior rate performance and cyclic stability. PDA-C/NiCo-LDH(cathode)//AC(anode) exhibited a high energy density of 62.7 W h kg^{-1} and exceptional cyclic performance of 10 000 cycles with a capacitance retention of 92.5%.[203] Gamma-phase Ni–Co oxyhydroxides were prepared and displayed a high electrical properties. Ni–Co oxyhydroxides//AC showed an ultra-high energy density of 92.6 W h kg^{-1} and capacitance retention of 91% after 7000 cycles.[204] NiCo-metal–organic frameworks (MOF) micro flowers possessed a high specific capacitance. Also, NiCo-P was prepared *via* a low-temperature phosphating method using the precursor of NiCo-MOF micro flowers. The NiCo-P(6) revealed the superior rate capability with the specific capacitances. NiCo-P(6)//AC supercapacitor exhibited a high energy density and outstanding cycling stability.[205] NiCo double hydroxide (NiCo-DH)/MOF was prepared and showed an electrode ultrahigh specific capacitances capacitance of 325.6 mA h g^{-1}. As a cathode for NiCo-Zn batteries, it exhibited high specific capacitances while the NiCo-DH//AC supercapacitor exhibited a remarkable performance.[206] A core-sheath of $MnCo_2O_4$/NiCo-layered double hydroxide (NiCo-LDH)/Ni foam ($MnCo_2O_4$/NiCo-LDH/NF) has been prepared and used as a cathode in supercapacitors that led to the specific capacitances of 4555.0 F g^{-1}. Also, the $MnCo_2O_4$/NiCo-LDH/NF//AC supercapacitor exhibited an outstanding energy density and can light up the green LED indicator for more than 30 min.[207] The ZnO/NiCo-LDH/carbon cloth (CC) is synthesized so that ZnO/NiCo-LDH300s shows excellent electrochemical performance. The supercapacitor of ZnO/NiCo-LDH300s//AC exhibited an energy density of 0.044 mW h cm^{-2}.[208]

In the production of NiCo-LDH (layered double hydroxide) nanosheets on an ultrathin $NiCoZnS_x$ (sulfide) microplate were prepared and exhibited a high specific capacitance of 1928 F g^{-1} and outstanding rate capability as well as a high energy density and good cycling stability of its supercapacitor with AC electrode.[209] NiCoP (phosphide) composites with carbon cloth (NiCoP@CC) and Co-based ZIF-67 (Co-ZIF-67) were prepared and the NiCoP@CC electrode showed a remarkable specific capacity of 1149.2 C g^{-1} and good traits. The supercapacitor of the NiCoP@CC cathode and AC as the anode delivered a high specific energy.[210] The hollow microcube of

NiCoP (phosphide) was synthesized (NiCoP-HMC) as an electrode and exhibited a remarkable specific capacity of 1088.9 C g^{-1}. Furthermore, an asymmetry supercapacitor was fabricated by using the NiCoP-HMCs of the (+) electrode and AC as the negative electrode with a high specific energy of 78.2 W h kg^{-1}.[211] Stable α-phase NiCoAl hydroxides were used in a NiCoAl-10 supercapacitor electrode with excellent specific capacitances of 19.27 F cm^{-2}. A supercapacitor of NiCoAl-10//AC also exhibited a remarkable energy density and capacity retention.[212] The hollow carbon-incorporated NiCoM layered double hydroxide nanocages (NiCoM-LDH/C, M = Mn, Cu, and Zn) are successfully synthesized and the optimized NiCoMn-LDH/C showed a meaningful capacity performance of 888.3 C g^{-1}. Also, the HSC device of NiCoMn-LDH/C and AC revealed a remarkable energy density of 46.5 W h kg^{-1} and capacitance retention of 92.05% after 5000 cycles.[213]

2.4.2. Ternary nickel cobalt sulfide/oxides and active carbon-based asymmetric supercapacitors. $NiCo_2S_4$ composites were prepared with citric acid as an inductive agent. Among the samples, $NiCo_2S_4$ mesoporous microspheres display the best electrochemical properties. Moreover, the $NiCo_2S_4$//AC supercapacitor yields an energy density of 48.7 W h kg^{-1}.[214] Tremella-like core-shellCo_9S_8/$NiCo_2S_4$/nickel foam (NF) was synthesized and the prepared Co_9S_8/$NiCo_2S_4$/NF electrode presents a high specific capacitance with a superior rate capability. Furthermore, the fabricated Co_9S_8/$NiCo_2S_4$/NF//AC supercapacitor displays a high energy density of 30 W h kg^{-1}.[215] The foam-structured $NiCo_2S_4$ (FSNCS) was synthesized by using the framework of the well-dispersed SiO_2 nanospheres. It exhibited 559.3 C g^{-1} at a current density of 1 A g^{-1} which was 173.3 C g^{-1} higher than the performance of the free SiO_2 NCS. The FSNCS//AC displays an energy density of 28.8 W h kg^{-1} with a good cyclic life of 88.9% after 5000 cycles.[216] The ultrathin and porous $NiCo_2O_4$ nanosheet-based electrodes were synthesized and exhibited a high area capacity of 2690 F g^{-1}. The corresponding supercapacitor if $NiCo_2O_4$(+)//(−)AC delivered a superior energy density of 52.6 W h kg^{-1} with a capacitance retention of 80.9% after 3000 cycles.[217] The (In)-doped $NiCo_2O_4$ (In-$NiCo_2O_4$) nanoneedles with oxygen vacancies (Vo) on the carbon fiber (CF) (In-$NiCo_2O_4$/CF) were synthesized using a simple laser-assisted technique. This electrode exhibited a high specific capacitance of 2375.1 F g^{-1} as well as the good parameters of the In-$NiCo_2O_4$/CF//AC supercapacitor.[218] $Ti_3C_2T_x$/$NiCo_2O_4$ (s-Ti_3C_2/$NiCo_2O_4$) were designed and used in the supercapacitors of s-Ti_3C_2/$NiCo_2O_4$ (+)//(−)AC with a widened voltage window of 1.6 V, which is almost twice wider than that of the common symmetric one. The device delivered high electrochemical performance.[219]

Graphene, CNTs, porous carbon, and nanomaterials are widely used in supercapacitor electrodes and industry.[220–222] Graphene-based supercapacitors leverage the unique properties of graphene, a single layer of carbon atoms, for energy storage. They offer a high power density, rapid charging, and discharging, a large surface area for increased energy storage, long cycle life, and environmental friendliness. Carbon nanomaterials offer a high surface area, nanoscale porosity, and excellent conductivity, providing efficient ion adsorption and increased capacitance. Ni materials are widely used in supercapacitor electrodes. They offer high capacitance, excellent conductivity, and electrochemical stability. These materials can store a substantial amount of charge, provide a high power performance, and exhibit a long cycle life. Incorporating Ni materials enhances energy storage capabilities, driving the development of high-performance devices. In summary, supercapacitor electrodes based on nickel material composites with graphene, CNTs, and porous carbon show acceptable electrochemical behavior. The porous CuNi phosphide spheres/rGO as the cathode electrode has advantages such as fast electrolyte diffusion, better electron transfer, and better structural stability. The holey graphene oxide (HGO)/nano two-dimensional Ni (Ni(BDC)-HGO30) indicated an energy density of 52.5 W h kg^{-1} and an excellent power density of 18 000 W kg^{-1}.[97] NiCo-based supercapacitors offer advantages such as high-power density, enabling them to deliver and absorb large amounts of energy quickly. They also have a long cycle life and good thermal stability, operating over a wide temperature range. The NiCo phosphide nano horns are formed by the Kirkendall effect for preparing the NiCo phosphide/phosphorus-doped rGO as an anode achieving an energy density of 39.7 W h kg^{-1} and a distinguished power density of 8820 W kg^{-1}.[105] An asymmetric supercapacitor based on the Fe-doped $NiCo_2O_4$/rGO electrode displayed an outstanding energy density of 93.5 W h kg^{-1} and specific capacitance of 2772 F g^{-1}.[128] The Ni phosphate (NiP)/MWCNTs revealed a superior energy density of 94.4 W h kg^{-1} at 340 W kg^{-1}.[148] Ni ferrite nanoparticle/carboxymethyl cellulose-derived porous carbon ($NiFe_2O_4$/CPC) exhibited a major energy density of 135.2 W h kg^{-1} at 10 040 W kg^{-1}.[172] A supercapacitor with Ti_3C_2Tx MXene/$NiCo_2O_4$//AC electrodes delivered a high electrochemical performance with energy and power densities of 94.46 W h kg^{-1} and 2882 W kg^{-1}, respectively.[219] A comparison of power density as a function of energy density for supercapacitors based on the Ni-materials/graphene, Ni-materials/CNTs, Ni-materials/porous carbon, and Ni-materials//active carbon structures is shown in Fig. 12. As can be seen from Fig. 9, the Ni-materials/graphene-based

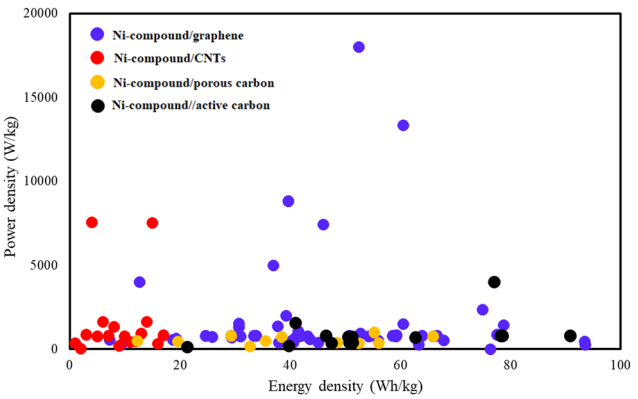

Fig. 12 Comparison of power density as a function of energy density for supercapacitors based on the Ni-materials/graphene, Ni-materials/CNTs, Ni-materials/porous carbon, and Ni-materials//active carbon structures.

supercapacitors have better power and energy densities of up to 10 kW kg^{-1} and 100 W h kg^{-1} respectively.

In this review the power and energy densities and specific capacitance of supercapacitors based on Ni cobalt/selenide and graphene composites, ternary nickel cobalt sulfide/oxides and graphene composites, $Ni(OH)_2$ anchored graphene, CNTs-based nickel composites, CNTs decorated with nickel cobalt, ternary nickel cobalt sulfide/oxides and CNT composites, and dispersion of Ni materials in porous carbon have been investigated. It seems that the comparison between recent advances in Ni materials/carbon nanocomposites shows that most of the supercapacitors are limited to the sub-region of 100 W h kg^{-1} and 5000 W kg^{-1}. The Ni compound/graphene-based supercapacitors achieve a higher power density than other nanocomposites of Ni materials and CNTs, porous carbon, and active carbon and they can overcome this limitation. Also, among the supercapacitors, Ni materials/graphene electrodes show a higher specific capacitance.

3. Conclusion

In conclusion, the appearance of supercapacitors based on Ni materials/graphene, Ni materials/CNTs, Ni materials/porous carbon, and Ni materials//active carbon has demonstrated significant advancements in energy storage. These innovative materials have enabled the development of supercapacitors with remarkable energy and power densities. These supercapacitors have achieved an impressive energy density of up to 10 kW kg^{-1}, allowing for efficient and long-lasting energy storage. This high energy density makes them suitable for diverse applications such as renewable energy systems, electric vehicles, and portable electronics. Moreover, these supercapacitors exhibit a power density of up to 100 W h kg^{-1}, enabling rapid energy release and meeting high power demands. This characteristic proves valuable in applications that require quick energy bursts, such as regenerative braking and power backup systems. This high specific capacitance ensures effective energy storage and swift charge–discharge cycles. The development of supercapacitors based on Ni-materials/graphene, Ni-materials/CNTs, Ni-materials/porous carbon, and Ni materials//active carbon has opened up new horizons for high-performance energy storage. With their impressive energy and power densities, along with their high specific capacitance, these supercapacitors hold great promise as a sustainable and efficient energy storage solution for the future.

Data Availability Statement

Data are contained within the article.

Conflicts of interest

The authors declare no conflicts of interest.

Acknowledgements

This research work was financially supported by East Tehran Branch, Islamic Azad University and the Iran National Science Foundation (INSF) and grant number (INSF: 97003234).

References

1 N. R. Chodankar, H. D. Pham, A. K. Nanjundan, J. F. S. Fernando, K. Jayaramulu, D. Golberg, Y. Han and D. P. Dubal, *Small*, 2020, **16**, e2002806.
2 O. Maurya, S. Khaladkar, M. R. Horn, B. Sinha, R. Deshmukh, H. Wang, T. Kim, D. P. Dubal and A. Kalekar, *Small*, 2021, **17**, 2300013.
3 S. M. Mahadik, N. R. Chodankar, Y. Han, D. P. Dubal and S. Patil, *ChemSusChem*, 2021, **14**, 5384–5398.
4 L. F. Aval, M. Ghoranneviss and G. B. Pour, *Heliyon*, 2018, **4**, e00862.
5 G. Behzadi pour, H. Nazarpour fard, L. Fekri aval and P. Esmaili, *Ionics*, 2019, **26**, 549–563.
6 Y. Tian, F. Yang, Z. Qiu, J. Jing, J. He and H. Xu, *J. Energy Storage*, 2023, **63**, 107086.
7 W. Wu, T. Liu, X. Zhang, C. Zhao, D. Yi, Y. Fang, J. Diwu, L. Wang and J. Zhu, *J. Mater. Sci.: Mater. Electron.*, 2023, **34**, DOI: **10.1007/s10854-023-10202-6**.
8 M. Zhang, D. Jiang, F. Jin, Y. Sun, J. Wang, M. Jiang, J. Cao, B. Zhang and J. Liu, *J. Colloid Interface Sci.*, 2023, **636**, 204–215.
9 V. Shanmugavalli, R. D. Kumar, A. J. Kumar, R. Kavitha, C. Brundha, V. Sampath and M. Lee, *J. Mater. Sci.: Mater. Electron.*, 2023, **34**, DOI: **10.1007/s10854-023-10248-6**.
10 R. Liu, J. Huang, Y. Diao, W. Zhao and H.-C. Chen, *J. Colloid Interface Sci.*, 2023, **639**, 263–273.
11 Z. Yuan, Y. Ma, P. Zhang, M. Zhai, C. Qin and X. Jiang, *Energy Fuels*, 2023, **37**, 2420–2430.
12 S. Jo, N. Kitchamsetti, H. Cho and D. Kim, *Polymers*, 2023, **15**, 454.
13 Y.-C. Hsiao, C.-H. Liao, C.-S. Hsu, S. Yougbaré, L.-Y. Lin and Y.-F. Wu, *J. Energy Storage*, 2023, **57**, 106171.
14 Y.-F. Wu, Y.-C. Hsiao, C.-H. Liao, C.-S. Hsu, S. Yougbaré and L.-Y. Lin, *J. Colloid Interface Sci.*, 2022, **628**, 540–552.
15 J. H. Kim, Y. Ko, S. Y. Lee, Y. S. Lee, S. K. Kim, Y. A. Kim and C. Yang, *Int. J. Energy Res.*, 2022, **46**, 23564–23577.
16 L. Wei, J. Li, R. Chen, Q. Wu and J. Li, *J. Nanopart. Res.*, 2022, **24**, DOI: **10.1007/s11051-022-05606-0**.
17 S. Su, L. Sun, J. Qian, X. Shi and Y. Zhang, *ACS Appl. Energy Mater.*, 2021, **5**, 685–696.
18 M. Jiang, Z. Hu, Y. Wang, C. Xiang, Y. Zou, F. Xu, Q. Yang, J. Zhang and L. Sun, *J. Alloys Compd.*, 2022, **927**, 166824.
19 J. Li, Y. Zou, L. Jin, F. Xu, L. Sun and C. Xiang, *J. Energy Storage*, 2022, **50**, 104639.
20 B. Huang, D. Yao, J. Yuan, Y. Tao, Y. Yin, G. He and H. Chen, *J. Colloid Interface Sci.*, 2022, **606**, 1652–1661.
21 Q. Xu, X. Liu, J. Zhang, Y. Xu, M. Zhou, J. Li, M. Du, K. Zhang, X. Qian, B. Xu, X. Wang, B. Wang and K. Zhang, *J. Mater. Chem. A*, 2023, **11**, 5309–5319.

22 C. Shi, J. Sun, Y. Pang, Y. Liu, B. Huang and B.-T. Liu, *J. Colloid Interface Sci.*, 2022, **607**, 462–469.
23 Y. J. Yang, S. Chen, C. Jiang, N. Wang, P. Yang, M. Liu and Y. Cheng, *J. Alloys Compd.*, 2023, **930**, 167466.
24 L. Xue'an, T. Liyi, Q. Jian, T. Dajiang, T. Zhangfa and Q. Huiying, *CIESC J.*, 2022, **73**, 3287–3297, DOI: **10.11949/0438-1157.20220391**.
25 C. Hou, T. Li, Z. Zhang, C. Chang and L. An, *Mater. Lett.*, 2022, **309**, 131361.
26 J. Chen, Z. Du, K. Cheng, J. Bao, G. Wang, Y. Yao, J. Song, J. Yue, K. Xu, W. Xie, W. Qiang, Y. Liu and X. Wang, *RSC Adv.*, 2022, **12**, 34904–34909.
27 S. Ramesh, K. Karuppasamy, D. Vikraman, H. M. Yadav, H.-S. Kim, A. Sivasamy and H. S. Kim, *Ceram. Int.*, 2022, **48**, 29102–29110.
28 J. Xiao, H. Tong, F. Jin, D. Gong, X. Chen, Y. Wu, Y. Zhou, L. Shen and X. Zhang, *J. Power Sources*, 2022, **518**, 230763.
29 G. B. Pour, H. Ashourifar, L. F. Aval and S. Solaymani, *Symmetry*, 2023, **15**, 1179.
30 M. B. Poudel, A. A. Kim, P. C. Lohani, D. J. Yoo and H. J. Kim, *J. Energy Storage*, 2023, **60**, 106713.
31 R. Wang, X. Li, Z. Nie, Y. Wang, Y. Zhao and H. Wang, *Energy Fuels*, 2022, **36**, 13256–13265.
32 Y. Fang, H. Wang, X. Wang, J. Ren and R. Wang, *Front. Chem. Sci. Eng.*, 2023, **17**, 373–386.
33 Z. Qin, J. Liu, B. Sun, H. Zou, L. Chen, Y. Xu, Y. Cao and C. Chen, *Electrochim. Acta*, 2022, **435**, 141370.
34 X. Dong, Z. Liu, H. Tan, P. Hu, Z. Zhang, Z. Huang and C. Shang, *Mater. Today Chem.*, 2022, **26**, 101234.
35 Y. Cao, N. Wu, F. Yang, M. Yang, T. Zhang, H. Guo and W. Yang, *Colloids Surf., A*, 2022, **646**, 128954.
36 B. Geng, W. Hu, X. Wu, M. Du, G. Shan and Q. Zheng, *J. Electrochem. Soc.*, 2022, **169**, 082521.
37 M. Liang, X. Li, Y. Kang, N. Ur RehmanLashari, X. Zhang, Y. Zhao, H. Wang, Z. Miao and C. Fu, *J. Power Sources*, 2022, **535**, 231486.
38 S. Ramesh, K. Karuppasamy, D. Vikraman, H. M. Yadav, H.-S. Kim, J.-H. Kim and H. S. Kim, *J. Energy Storage*, 2022, **55**, 105728.
39 M. Pathak and C. S. Rout, *Adv. Compos. Hybrid Mater.*, 2022, **5**, 1404–1422.
40 L. Cui, H. Xu, Y. An, M. Xu, Z. Lei and X. Jin, *New J. Chem.*, 2022, **46**, 12419–12426.
41 D. N. Sangeetha, M. Selvakumar, P. Selvaraj and S. Senthilkumar, *Mater. Lett.*, 2022, **313**, 131765.
42 M. Pathak, S. R. Polaki and C. S. Rout, *RSC Adv.*, 2022, **12**, 10788–10799.
43 M. Ding, Z. Wei, S. Huang, C. Li and Q. Lu, *Current Nanoscience*, 2022, **18**, 399–407.
44 X. Wang, C. Deng, X. Hong, W. Dong and B. Liang, *J. Energy Storage*, 2022, **55**, 105837.
45 K. Venkatesh, C. Karuppiah, R. Palani, G. Periyasamy, S. K. Ramaraj and C.-C. Yang, *Mater. Lett.*, 2022, **323**, 132609.
46 H. Zhang, J. Han, J. Xu, Y. Ling and X. Ou, *J. Mater. Sci.*, 2022, **57**, 5566–5576.
47 Y. Tian, Z. Xue, Q. Zhao, J. Guo, K. Tao and L. Han, *Dalton Trans.*, 2022, **51**, 4406–4413.
48 T. Kavinkumar, N. Naresh, G. Mathew and B. Neppolian, *J. Alloys Compd.*, 2022, **891**, 162052.
49 B. Deng, Y. Yang, Y. Liu, B. Yin and M. Yang, *J. Colloid Interface Sci.*, 2022, **618**, 399–410.
50 M. Aghazadeh and H. F. Rad, *J. Mater. Sci.: Mater. Electron.*, 2022, **33**, 11038–11054.
51 J. Fan, A. Chen, X. Xie and L. Gu, *J. Energy Storage*, 2022, **48**, 103964.
52 X. Liu and J. Xie, *J. Mater. Sci.: Mater. Electron.*, 2022, **33**, 4081–4092.
53 J. R. Junaqani, M. Kazazi, M. J. S. Shahraki and M. D. Chermahini, *JOM*, 2022, **74**, 808–816.
54 X. Liu, S. Du, X. Zuo, X. Zhang and Y. Jiang, *RSC Adv.*, 2022, **12**, 1177–1183.
55 G. B. Pour, L. F. Aval and M. Mirzaee, *Nanotechnology*, 2020, **14**, 163–170.
56 T. Chen and L. Dai, *Mater. Today*, 2013, **16**, 272–280.
57 Y. Wu, X. Jia, H. Zhang, F. Zhou, Z. Fu, X. Jia, Z. Li, F. Liu, L. Wang and Z. Xiao, *J. Energy Storage*, 2023, **62**, 106855.
58 R. Ghanbari and S. R. Ghorbani, *J. Energy Storage*, 2023, **60**, 106670.
59 M. Miah, P. Hota, T. K. Mondal, R. Chen and S. K. Saha, *J. Alloys Compd.*, 2023, **933**, 167648.
60 M. Li, C. Jia, D. Zhang, Y. Luo, Y. Ma, G. Luo, L. Zhao, L. Wang, Z. Li, Q. Lin, P. Yang, N. Zhu, R. Boukherroub and Z. Jiang, *J. Energy Storage*, 2023, **64**, 107144.
61 Y. Abbasi, F. Jalali and S. Sheikhi, *J. Alloys Compd.*, 2023, **938**, 168450.
62 A. Agarwal, S. Majumder and B. R. Sankapal, *J. Energy Storage*, 2023, **58**, 106396.
63 E. Baasanjav, T. G. Senthamaraikannan, P. Bandyopadhyay, D.-H. Lim and S. M. Jeong, *Chem. Eng. J.*, 2023, **466**, 143064.
64 H. Lv, Z. Xiao, S. Zhai, X. Wang, J. Hao, Y. Tong and Q. An, *Ind. Crops Prod.*, 2023, **194**, 116320.
65 S. Demirel, M. S. Nas, A. Kocyigit, M. H. Calimli and M. H. Alma, *J. Mater. Sci.: Mater. Electron.*, 2023, **34**, DOI: **10.1007/s10854-023-09894-7**.
66 X. Sun, Y. Liu, Z. Xu, X. Gao, X. Yin and X. Ma, *Phys. Chem. Chem. Phys.*, 2022, **24**, 29817–29826.
67 R. Liu, X.-R. Shi, Y. Wen, X. Shao, C. Su, J. Hu and S. Xu, *J. Energy Chem.*, 2022, **74**, 149–158.
68 Y. Li, G. Huang, Q. Geng, Y. Liu, X. Li, Y. Yao, Y. Liu, B. Xing, Q. Liu, J. Jia and C. Zhang, *J. Alloys Compd.*, 2022, **895**, 162652.
69 L. F. Aval, M. Ghoranneviss and G. B. Pour, *Mater. Renew. Sustainable Energy*, 2018, 7.
70 Y. F. Avval, G. B. Pour and M. M. Aram, *Int. Nano Lett.*, 2022, **12**, 421–426.
71 C.-Y. Hsu, A. M. Rheima, Z. Sabri Abbas, M. U. Faryad, M. M. Kadhim, U. S. Altimari, A. H. Dawood, A. Dhari jawad al-bayati, Z. T. Abed, R. S. Radhi, A. S. Jaber, S. K. Hachim, F. K. Ali, Z. H. Mahmoud, G. Behzadi Pour and E. Kianfar, *S. Afr. J. Chem. Eng.*, 2023, **46**, 286–311.

72 S. Khatami, G. B. Pour, S. F. Aval and M. Amini, *Plasma Chem. Plasma Process.*, 2023, **43**, 1131–1147.
73 A. K. Alkhawaldeh, A. M. Rheima, M. M. Kadhim, Z. Sabri Abbas, A. Dhari Jawad al-Bayati, Z. Talib Abed, F. Mohamed Dashoor Al-Jaafari, A. Salam Jaber, S. K. Hachim, F. K. Ali, Z. H. Mahmoud, G. Behzadi Pour and E. Kianfar, *Case Stud. Chem. Environ. Eng.*, 2023, **8**, 100372.
74 S. Khatami, L. Fekri Aval and G. Behzadi Pour, *NANO*, 2018, **13**, 1850062.
75 G. Behzadi Pour and L. Fekri Aval, *Micro Nano Lett.*, 2018, **13**, 149–153.
76 T. Nandagopal, G. Balaji and S. Vadivel, *J. Electroanal. Chem.*, 2023, **928**, 116944.
77 J. Acharya, B. Pant, G. Prasad Ojha and M. Park, *J. Colloid Interface Sci.*, 2022, **610**, 863–878.
78 S. Sardana, K. Aggarwal, S. Malik, A. Saini, S. Dahiya, R. Punia, A. S. Maan, K. Singh and A. Ohlan, *Electrochim. Acta*, 2022, **434**, 141324.
79 B. Carmel Jeeva Mary, J. J. Vijaya, B. Saravanakumar, M. Bououdina and L. J. Kennedy, *Synth. Met.*, 2022, **291**, 117201.
80 M. Amiri, A. Mohammadi Zardkhoshoui and S. S. Hosseiny Davarani, *Nanoscale*, 2023, **15**, 2806–2819.
81 M. Amiri, A. Mohammadi Zardkhoshoui and S. S. Hosseiny Davarani, *Nanoscale*, 2023, **15**, 2806–2819.
82 Q. Yang, Q. Feng, X. Xu, Y. Liu, X. Yang, F. Yang, J. Li, H. Zhan, Q. Wang and S. Wu, *Nanotechnology*, 2022, **33**, 345401.
83 M. Farshadnia, A. A. Ensafi, K. Zarean Mousaabadi and B. Rezaei, *J. Alloys Compd.*, 2022, **906**, 164278.
84 Y. Cui, C. Zhao, L. Zhao, H. Yu, J. Wang and Z. Zhang, *Diamond Relat. Mater.*, 2022, **125**, 108965.
85 M. Imranullah, T. Hussain, R. Ahmad, U. Shuaib, P. O. Agboola and I. shakir, *Ceram. Int.*, 2022, **48**, 12460–12466.
86 S. Ghosh, P. Samanta, W. Jang, C.-M. Yang, N. C. Murmu and T. Kuila, *ACS Appl. Energy Mater.*, 2022, **5**, 1528–1541.
87 B. A. Khan, R. Hussain, A. Shah, A. Mahmood, M. Z. U. Shah, J. Ismail, S. Ur Rahman, M. Sajjad, M. A. Assiri, M. Imran and M. S. Javed, *Ceram. Int.*, 2022, **48**, 5509–5517.
88 J. Wang, S. Li, Y. Zhu, S. Zhai, C. Liu, N. Fu, S. Hou, Y. Niu, J. Luo, S. Mu and Y. Huang, *J. Electroanal. Chem.*, 2022, **919**, 116548.
89 R. Xiong, X. Zhang, X. Xu, Z. Zhang, X. Tian and C. Wang, *Diamond Relat. Mater.*, 2022, **127**, 109183.
90 X. Shi, Q. Liu, W. Liang, B. Chen, L. Shao, J. Cai, Z. Sun, Y. Zhang, H. Huang and Y. Wu, *Mater. Today Sustainability*, 2022, **18**, 100151.
91 Z. Lu, H. Zhao, J. Luo and J. Wang, *J. Phys. Chem. Solids*, 2022, **163**, 110593.
92 J. Miao, D. Wu, X. Gao, W. Wang, W. Wu, S. Tao, Y. Fang, Z. Han, B. Qian, X. Jiang and L. Zhang, *J. Alloys Compd.*, 2022, **890**, 161435.
93 C. Li, G. Jiang, T. Liu, Z. Zeng, P. Li, R. Wang and X. Zhang, *J. Energy Storage*, 2022, **49**, 104176.
94 V. M. Maphiri, D. T. Bakhoum, S. Sarr, N. F. Sylla, G. Rutavi and N. Manyala, *J. Energy Storage*, 2022, **52**, 104967.
95 A. Morenghi, S. Scaravonati, G. Magnani, M. Sidoli, L. Aversa, R. Verucchi, G. Bertoni, M. Riccò and D. Pontiroli, *Electrochim. Acta*, 2022, **424**, 140626.
96 Y. Jia, D. Hu, X. Wang, H. Zhang and P. Du, *J. Energy Storage*, 2022, **50**, 104713.
97 H. Wang, P. Zhao, X. Zhang, S. Zhang, X. Lu, Z. Qiu, K. Ren, Z. Xu, R. Yao, T. Wei and Z. Fan, *Nano Res.*, 2022, **15**, 9047–9056.
98 K. K. Sarigamala, A. Struck, S. Shukla and S. Saxena, *Electrochim. Acta*, 2023, **450**, 142266.
99 M. Hammad Aziz, F. Shaheen, R. Ahmad, A. Khan, S. Sharif, H. Muhammad Fahad and Q. Huang, *Mater. Lett.*, 2023, **333**, 133658.
100 C. Li, G. Zhang, X. Li, H. Wang, P. Huo and X. Wang, *J. Phys. Chem. Solids*, 2022, **163**, 110591.
101 Q. Luo, Z. Zhong, Y. Zheng, D. Gao, Z. Xia and L. Wang, *Talanta*, 2021, **224**, 121869.
102 A. B. Ganganboina and R.-A. Doong, *Environ. Sci.: Nano*, 2020, **7**, 228–237.
103 P. Rosaiah, N. G. Prakash, P. Divya, S. Sambasivam, M. Shkir, H. Algarni and T. J. Ko, *J. Energy Storage*, 2022, **56**, 106133.
104 A. G. El-Deen, M. K. Abdel-Sattar and N. K. Allam, *Appl. Surf. Sci.*, 2022, **587**, 152548.
105 U. Javed, G. Dhakal, A. M. Rabie, S. Iqbal, Y. R. Lee, J. Lee and J.-J. Shim, *Mater. Today Nano*, 2022, **18**, 100195.
106 T. Zhou, S. Tang, H. Yu, L. Shen, Q. Huang, S. Yang, L. Yu and L. Zhang, *New J. Chem.*, 2022, **46**, 10328–10338.
107 Y. Wang, F. Mo and X. Wu, *J. Electroanal. Chem.*, 2022, **924**, 116863.
108 Y. Zhou, L. Wei, C. Li, Y. Han, J. Xu, Z. Jia, J. Sun, H. Chen, Y. Song, X. Ouyang, X. Wang, J. Zhu and Y. Fu, *J. Energy Storage*, 2022, **45**, 103765.
109 X. Yin, L. Han, Y. Fu, J. Lu, Q. Song and H. Li, *J. Energy Storage*, 2022, **53**, 105205.
110 J. Zou, D. Xie, J. Xu, X. Song, X. Zeng, H. Wang and F. Zhao, *Appl. Surf. Sci.*, 2022, **571**, 151322.
111 X. Wang, Y. Xu, L. Shao, Y. Wei, X. Zhang, X. An, J. Liu, C. Zhou, Y. Chen and G. Wang, *J. Energy Storage*, 2023, **63**, 107056.
112 L. Chen, X. Zhao, G. Tian, Y. Wei and T. Liu, *Mater. Lett.*, 2023, **334**, 133698.
113 C. Li, G. Jiang, M. Demir, Y. Sun, R. Wang and T. Liu, *J. Energy Storage*, 2022, **56**, 105986.
114 G. Rutavi, D. J. Tarimo, V. M. Maphiri and N. Manyala, *Int. J. Energy Res.*, 2022, **46**, 11214–11227.
115 T. Zhao, C. Liu, T. Meng, W. Deng, L. Zheng, F. Yi, A. Gao and D. Shu, *Small*, 2022, **18**, 2201286, DOI: 10.1002/smll.202201286.
116 H. Qiu, Q. Ma, X. Sun, X. Han, G. Jia, Y. Zhang and W. He, *Appl. Surf. Sci.*, 2022, **578**, 152019.
117 Y. Liu, X. Li, M. Gao, X. Hao, J. Li, Y. Liu, Y. Li and K. Cai, *ACS Appl. Energy Mater.*, 2022, **5**, 9605–9615.
118 S. Khaladkar, G. Gund, O. Maurya, B. Sinha, P. Salame, D. Dubal, R. Deshmukh and A. Kalekar, *Adv. Energy Sustainability Res.*, 2023, 4.

119 S. R. Khaladkar, O. Maurya, G. Gund, B. Sinha, D. Dubal, R. R. Deshmukh and A. Kalekar, *J. Energy Chem.*, 2023, **87**, 304–313.
120 N. J. Panicker, J. C. Dutta and P. P. Sahu, *Chem. Eng. J.*, 2023, **463**, 142376.
121 X. Zang, L. Liang, X. Wang, C. Li, P. Li, Q. Shao and N. Cao, *Energy Technol.*, 2022, **10**, 2200490, DOI: **10.1002/ente.202200490**.
122 C. Cheng, Y. Zou, F. Xu, C. Xiang, Q. Sui, J. Zhang, L. Sun and Z. Chen, *J. Energy Storage*, 2022, **52**, 105049.
123 Y. Guo, C. Hao, X. Wang, Y. Yang, X. Wang, J. Wu and Y. Shen, *Ceram. Int.*, 2022, **48**, 17644–17653.
124 D. He, F. Li, Y. Xiao, S. Chen, Z. Zhu, H. Chen, X. Hu, W. Peng, S. Xin and Y. Bai, *Electrochim. Acta*, 2022, **404**, 139751.
125 A. I. Abdel-Salam, S. Y. Attia, F. I. El-Hosiny, M. A. Sadek, S. G. Mohamed and M. M. Rashad, *Mater. Chem. Phys.*, 2022, **277**, 125554.
126 S. Yadav, A. S. Ghrera and A. Devi, *J. Energy Storage*, 2022, **56**, 105949.
127 X. Chen, N. Xin, Y. Li, C. Sun, L. Li, Y. Ying, W. Shi and Y. Liu, *J. Mater. Sci. Technol.*, 2022, **127**, 236–244.
128 R. Nasser, X.-L. Wang, A. B. G. Trabelsi, F. H. Alkallas, H. Elhouichet and J.-M. Song, *J. Energy Storage*, 2022, **52**, 104619.
129 S. Pappu, S. Anandan, T. N. Rao, S. K. Martha and S. V. Bulusu, *J. Energy Storage*, 2022, **50**, 104598.
130 R. Yuan, W. Chen, J. Zhang, L. Zhang, H. Ren, T. Miao, Z. Wang, K. Zhan, M. Zhu and B. Zhao, *Dalton Trans.*, 2022, **51**, 4491–4501.
131 Z. Shi, G. Sun, R. Yuan, W. Chen, Z. Wang, L. Zhang, K. Zhan, M. Zhu, J. Yang and B. Zhao, *J. Mater. Sci. Technol.*, 2022, **99**, 260–269.
132 Y. Jiang, X. Li, F. Liu, B. Wang, W. Zhou, S. Dong and X. Fan, *Appl. Surf. Sci.*, 2022, **576**, 151801.
133 M.-J. Zeng, X. Li, S.-M. Hao, J. Qu, W. Li, J. Wu, T. Zhao and Z.-Z. Yu, *New J. Chem.*, 2022, **46**, 533–541.
134 J. Barqi, S. M. Masoudpanah, M. Hasheminiasari and X. Liu, *J. Alloys Compd.*, 2023, **930**, 167509.
135 C. Fang and D. Zhang, *J. Electrochem. Soc.*, 2022, **169**, 060528.
136 A. Viswanathan and A. N. Shetty, *J. Energy Storage*, 2023, **65**, 107337.
137 B. Guo, Y. Gao, Y. Li, X. Sun, S. Chen and M. Li, *ACS Appl. Nano Mater.*, 2022, **5**, 7471–7480.
138 R. Jafer, S. A. Alsufyani, J. Iqbal, M. O. Ansari, A. Numan, S. Bashir, P. M. Z. Hasan and S. Wageh, *Polymers*, 2023, **15**, 1267.
139 X. Wu, F. Zeng, X. Song, X. Sha, H. Zhou, X. Zhang, Z. Liu, M. Yu and C. Jiang, *Chem. Eng. J.*, 2023, **456**, 140947.
140 A. Rahmanian and L. Naji, *Colloids Surf., A*, 2022, **640**, 128450.
141 X. Wu, F. Zeng, X. Song, X. Sha, H. Zhou, X. Zhang, Z. Liu, M. Yu and C. Jiang, *Chem. Eng. J.*, 2023, **456**, 140947.
142 J. Li, H. Hao, J. Wang, W. Li and W. Shen, *J. Alloys Compd.*, 2019, **782**, 516–524.
143 J. Tian, Q. Shan, X. Yin and W. Wu, *Adv. Powder Technol.*, 2019, **30**, 3118–3126.
144 K. Yousefipour, R. Sarraf-Mamoory and A. Chaychi Maleki, *J. Energy Storage*, 2023, **59**, 106438.
145 M. W. Iqbal, M. H. Khan, A. M. Afzal, H. Hassan, H. A. Alzahrani and S. Aftab, *J. Appl. Electrochem.*, 2022, **53**, 949–962.
146 D. Zhang, M. Zhao, H. Zhang, M. Terrones and Y. Wang, *Carbon*, 2023, **201**, 1081–1089.
147 Y. Wang, M. Li, R. Ramachandran, H. Shan, Q. Chen, A. Luo, F. Wang and Z.-X. Xu, *J. Energy Chem.*, 2023, **76**, 214–225.
148 W. Shehzad, M. R. A. Karim, M. Z. Iqbal, N. Shahzad and A. Ali, *J. Energy Storage*, 2022, **54**, 105231.
149 Y. Hao, H. Guo, F. Yang, J. Zhang, N. Wu, M. Wang, C. Li and W. Yang, *J. Alloys Compd.*, 2022, **911**, 164726.
150 S. Su, L. Sun, F. Xie, J. Qian and Y. Zhang, *Front. Chem. Sci. Eng.*, 2023, **17**, 491–503.
151 Y. Chen, H. Hou, B. Liu, M. Li, L. Chen, C. Chen, S. Wang, Y. Li and D. Min, *Chem. Eng. J.*, 2023, **454**, 140453.
152 M. Huang, K. Zhao, D. He, J. He and Y. Wang, *Energy Fuels*, 2022, **36**, 15234–15243.
153 M. Zhao, H. Zhang, S. Zhai, L. Sun, Z. Huang, M. Guo, Y. Liu, D. Zhang, M. Terrones and Y. Wang, *J. Alloys Compd.*, 2022, **909**, 164664.
154 J. Qian, L. Sun, X. Shi, L. Wu, S. Su, K. Wang and Y. Zhang, *Chem. Eng. J.*, 2022, **429**, 132482.
155 Z. Shi, X. Xu, P. Jing, B. Liu and J. Zhang, *ACS Appl. Mater. Interfaces*, 2023, **15**, 7263–7273.
156 Y. Yuan, P. Cui, J. Liu, W. Ding, Y. Wang and L. Lv, *Molecules*, 2022, **27**, 7507.
157 J. Chen, Z. Du, K. Cheng, J. Bao, G. Wang, Y. Yao, J. Song, J. Yue, K. Xu, W. Xie, W. Qiang, Y. Liu and X. Wang, *RSC Adv.*, 2022, **12**, 34904–34909.
158 Z. Tian, D. Wang, C. Zhang, F. Meng, L. Cao and H. Lin, *J. Mater. Sci.*, 2022, **57**, 19381–19395.
159 M. Yao, X. Ji, X. Ou, P. Wu and S. Cheng, *J. Power Sources*, 2022, **543**, 231829.
160 T. Feng, H. Jiao, H. Li, J. Wang, S. Zhang and M. Wu, *Energy Fuels*, 2022, **36**, 2189–2201.
161 C. Hou, H. Wang, T. Li, Z. Zhang, C. Chang and L. An, *Chem. Res. Chin. Univ.*, 2022, **43**, 20220351, DOI: **10.7503/cjcu20220351**.
162 B. Q. Wang, S. H. Gong, Q. S. Sun, F. Liu, X. C. Wang and J. P. Cheng, *Electrochim. Acta*, 2022, **402**, 139575.
163 Z. Yang, X. Yang, T. Yang, Y. Cao, C. Zhang, Y. Zhang, P. Li, J. Yang, Y. Ma and Q. Li, *Energy Storage Mater.*, 2023, **54**, 51–59.
164 S. Khan Abdul, K. Anuj, F. Amjad, T. Mohammad, A. Muhammad, U. Muhammad, A. Akmal, A. Saira, P. Lujun and Y. Ghulam, *J. Energy Storage*, 2022, **56**, 106041.
165 X. Wang, X. Han, M. Lim, N. Singh, C. L. Gan, M. Jan and P. S. Lee, *J. Phys. Chem. C*, 2012, **116**, 12448–12454.
166 N. J. Panicker, J. C. Dutta and P. P. Sahu, *Chem. Eng. J.*, 2023, **463**, 142376.

167 J. Feng, X. Zhang, Q. Lu, E. Guo and M. Wei, *Energy Fuels*, 2022, **36**, 5424–5432.
168 C. Han, X. Ding and J. Zhu, *Ionics*, 2023, **29**, 1199–1207.
169 C. Wang, G. Sui, D. Guo, J. Li, X. Ma, Y. Zhuang and D.-F. Chai, *J. Energy Storage*, 2022, **50**, 104280.
170 J. Zhu, Q. Zhang, Y. Zhao, R. Zhang, L. Liu and J. Yu, *Carbon*, 2023, **202**, 13–25.
171 J. Yang, H. Li, S. He, H. Du, K. Liu, C. Zhang and S. Jiang, *Polymers*, 2022, **14**, 2521.
172 H. Lv, Z. Xiao, S. Zhai, J. Hao, Y. Tong, G. Wang and Q. An, *J. Colloid Interface Sci.*, 2022, **622**, 327–335.
173 T. Yan, M. Wang, K. Li, X. Ni, X. Du, M. Xi, H. Chen and A. Ju, *J. Alloys Compd.*, 2022, **898**, 162834.
174 Z. Yuan, Y. Ma, P. Zhang, M. Zhai, C. Qin and X. Jiang, *Energy Fuels*, 2023, **37**, 2420–2430.
175 K. Zhao, X. Sun, Z. Wang, C. Huang, D. Li and J. Liu, *J. Alloys Compd.*, 2022, **921**, 166036.
176 D.-Y. Kim, C.-H. Ma, Y. Jang, S. Radhakrishnan, T. H. Ko and B.-S. Kim, *Colloids Surf., A*, 2022, **652**, 129785.
177 Z.-W. Zhang, C.-Y. Lu, G.-H. Liu, Y.-J. Cao, Z. Wang, T. Yang, Y.-H. Kang, X.-Y. Wei and H.-C. Bai, *J. Mater. Res. Technol.*, 2022, **19**, 3034–3045.
178 Y. Hou, Q. Sun and H. Du, *J. Alloys Compd.*, 2023, **937**, 168399.
179 Y. Wang, Y. Liu, Z. Chen, M. Zhang, B. Liu, Z. Xu and K. Yan, Green, *Chem. Eng.*, 2022, **3**, 55–63.
180 O. P. Nanda, A. G. Prince, L. Durai and S. Badhulika, *Energy Fuels*, 2023, **37**, 4701–4710.
181 R. S. Karmur, D. Gogoi, M. R. Das and N. N. Ghosh, *Energy Fuels*, 2022, **36**, 8488–8499.
182 G. Wang, Z. Xu, Z. Li, Y. Ding, R. Ge, M. Xiang, G. Wang and Z. Yan, *Electrochim. Acta*, 2023, **443**, 141980.
183 G. Wang, K. Qi, Z. Yan, L. Yue, Y. Ding, W. Li and Z. Xu, *Appl. Surf. Sci.*, 2022, **592**, 153293.
184 X. Ren, Z. Gan, M. Sun, Q. Fang, Y. Yan, Y. Sun, J. Huang, B. Cao, W. Shen, Z. Li and Y. Fu, *Electrochim. Acta*, 2022, **414**, 140208.
185 T. Hu, L. Gao, W. Zhou and J. Zhang, *J. Alloys Compd.*, 2022, **895**, 162577.
186 Y. He, T. Liu, J. Song, Y. Wang, Y. Zhang, J. Feng, A. Meng, G. Li, L. Wang, J. Zhao and Z. Li, *J. Energy Chem.*, 2023, **78**, 37–46.
187 Y. Lin, X. Chen, P. Chang, Z. Liu, G. Ren and J. Tao, *J. Alloys Compd.*, 2022, **900**, 163503.
188 Q. Fang, M. Sun, X. Ren, Y. Sun, Y. Yan, Z. Gan, J. Huang, B. Cao, W. Shen, Z. Li and Y. Fu, *J. Colloid Interface Sci.*, 2022, **611**, 503–512.
189 Z. Li, J. Ren, C. Yang, Y. He, Y. Liang, J. Liu, G. I. N. Waterhouse, J. Li and D. Qian, *J. Alloys Compd.*, 2021, **889**, 161661.
190 Z. Qin, Y. Xu, L. Liu, M. Liu, H. Zhou, L. Xiao, Y. Cao and C. Chen, *RSC Adv.*, 2022, **12**, 29177–29186.
191 R. Liang, Y. Du, J. Lin, J. Chen and P. Xiao, *Energy Fuels*, 2022, **36**, 7115–7120.
192 H. Li, X. Wang, L. Dai, F. Guo, H. Mi, C. Ji and L. Sun, *Inorg. Chem.*, 2022, **61**, 3866–3874.
193 D. P. Luo, Y. H. Chen, Y. B. Chen, Z. H. Wei, L. Zhang, X. Y. Ye, Q. T. Wang and L. A. Ma, *Mater. Lett.*, 2023, **333**, 133611.
194 B. Tao, W. Yang, M. Zhou, L. Qiu, S. Lu, X. Wang, Q. Zhao, Q. Xie and Y. Ruan, *J. Colloid Interface Sci.*, 2022, **621**, 139–148.
195 Y. Luan, H. Zhang, F. Yang, J. Yan, K. Zhu, K. Ye, G. Wang, K. Cheng and D. Cao, *Appl. Surf. Sci.*, 2018, **447**, 165–172.
196 J. Yang, C. Yu, X. Fan, S. Liang, S. Li, H. Huang, Z. Ling, C. Hao and J. Qiu, *Energy Environ. Sci.*, 2016, **9**, 1299–1307.
197 T. Dai, B. Cai, X. Yang, Y. Jiang, L. Wang, J. Wang, X. Li and W. Lü, *Nanotechnology*, 2023, **34**, 225401.
198 W. Zhao, X. Xu, N. Wu, X. Zhao and J. Gong, *Nanomaterials*, 2023, **13**, 730.
199 X. Chen, H. Li, J. Xu, F. Jaber, F. Musharavati, E. Zalnezhad, S. Bae, K. S. Hui, K. N. Hui and J. Liu, *Nanomaterials*, 2020, **10**, 1292.
200 Y. Guo, C. Hao, Y. Yang, X. Wu, C. Ni, X. Wang and X. Wang, *Ceram. Int.*, 2022, **48**, 9558–9568.
201 S.-C. Hsu, H.-H. Chiang, T.-Y. Huang, S.-H. Chao, R. T. Wu, C.-Z. Lu, J.-H. Huang, C.-W. Chang-Jian, H. C. Weng and H.-C. Chen, *Electrochim. Acta*, 2022, **403**, 139692.
202 C. Chen, M. Liu, Z. Liu, M. Xie, L. Wan, J. Chen, Y. Zhang, C. Du and D. Li, *J. Colloid Interface Sci.*, 2022, **614**, 66–74.
203 M. Fu, Z. Zhang, W. Chen, Y. Huang and H. Yu, *J. Alloys Compd.*, 2023, **938**, 168527.
204 X. Ren, M. Li, L. Qiu, X. Guo, F. Tian, G. Han, W. Yang and Y. Yu, *J. Mater. Chem. A*, 2023, **11**, 5754–5765.
205 Y. Cao, N. Wu, C. Li, Y. Chen, H. Zhang, H. Guo and W. Yang, *Colloids Surf., A*, 2023, **658**, 130683.
206 W. Wang, Y. Fang, S. Wang, Z. Zhang, R. Zhao and W. Xue, *J. Alloys Compd.*, 2022, **900**, 163532.
207 Y. Wang, Z. Wang, X. Zheng, X. Teng, L. Xu, Y. Yuan, X. Liu, A. Fu, Y. Li and H. Li, *J. Alloys Compd.*, 2022, **904**, 164047.
208 Y. B. Chen, L. A. Ma, X. Zhang, L. K. Huang, H. X. Chen and Q. T. Wang, *Mater. Technol.*, 2021, **37**, 1146–1155.
209 W. Hu, L. Chen, B. Geng, M. Du, G. Shan, Y. Song, Z. Wu and Q. Zheng, *ACS Appl. Energy Mater.*, 2023, **6**, 2781–2792.
210 X. Chen and J. Zhu, *J. Energy Storage*, 2022, **55**, 105877.
211 X. Chen and Y. Zhuang, *Dalton Trans.*, 2022, **51**, 16017–16026.
212 Z. Xu, X. Li, S. Sun, X. Wang, Z. Zhang, H. Li and S. Yin, *J. Power Sources*, 2022, **546**, 231982.
213 Z. Sheng, X. Lin, H. Gao, L. Huang, Y. Zhang, Y. Zhao, H. Wei, C. Wang, D. Xu and Y. Wang, *Int. J. Hydrogen Energy*, 2022, **47**, 29195–29206.
214 H. Xu, P. Chen, Y. Zhu, Y. Bao, J. Ma, X. Zhao and Y. Chen, *J. Electroanal. Chem.*, 2022, **921**, 116688.

215 Y. Yang, D. Qian, H. Zhu, Q. Zhou, Z. Zhang, Z. Li and Z. Hu, *J. Alloys Compd.*, 2022, **898**, 162850.
216 J. Wang, J. Wang, G. Zhu, H. Xu, X. Zhang, Y. Zhao, J. Zhang, K. Jiang and A. Yu, *J. Energy Storage*, 2022, **46**, 103907.
217 F. Ren, Z. Tong, S. Tan, J. Yao, L. Pei, Y. Ji and A. Abulizi, *J. Electrochem. Energy Convers. Storage*, 2021, **19**, 011004.
218 X. Luo, Q. Zhou, M. Guo, X. Peng, D. Wu, Y. Ito and Y. Liu, *Chem. Eng. J.*, 2022, **431**, 134220.
219 L. Wang, J. Cao, Y.-H. Zhou and X. Liu, *J. Electroanal. Chem.*, 2022, **923**, 116787.
220 G. Behzadi Pour, E. Shajee Nia, E. Darabi, L. Fekri Aval, H. Nazarpour-Fard and E. Kianfar, *Case Stud. Chem. Environ. Eng.*, 2023, **8**, 100527.
221 L. F. Aval and S. M. Elahi, *Electron. Mater. Lett.*, 2016, **13**, 77–85.
222 E. Akbarnejad, Z. Ghorannevis, E. Mohammadi and L. Fekriaval, *J. Electroanal. Chem.*, 2019, **849**, 113358.